Synthesis and studies on discrete copper halide clusters derived from pyridyl functionalized P-N ligands

A thesis submitted towards the partial fulfillment of

BS-MS Dual Degree Programme

by

SAURABH

(Reg. no. 20111013)

Under the guidance of

Dr. R. BOOMI SHANKAR

Indian Institute of Science Education and Research, Pune

Certificate

This is to certify that this dissertation entitled **"Synthesis and studies on discrete copper halide clusters derived from pyridyl functionalized P-N ligands"** towards the partial fulfilment of the **BS-MS dual degree programme** at the Indian Institute of Science Education and Research, Pune represents the research carried out by **Saurabh** at IISER Pune under the supervision of **Dr. R. Boomi Shankar**, Associate Professor at IISER Pune during the academic year 2015-2016.

R. Boomi Shankar.

Signature of the Supervisor

Date: 26/04/2016

Dr. R. Boomi Shankar

Associate Professor
Department of Chemistry
IISER Pune
Email: boomi@iiserpune.ac.in
Phone: 020-2590-8208

Declaration

I hereby declare that the matter embodied in the thesis entitled **"Synthesis and studies on discrete copper halide clusters derived from pyridyl functionalized P-N ligands"** are the results of the investigations carried out by me at the Department of Chemistry, Indian Institute of Science Education and Research Pune, under the supervision of Dr. R. Boomi Shankar and the same has not been submitted elsewhere for any other degree.

Saurabh

Signature of the Student

Date: 26/4/16

Saurabh

Regd. ID 20111013
IISER Pune

Acknowledgements

I would like to express my special thanks of gratitude to my advisor Dr. R. Boomi Shankar for his continuous support for my final year project. His motivation, enthusiasm, immense knowledge, and patience has always motivated me during my entire project. I could not have imagined having a better mentor for my final year M.S. project.

Besides my advisor, I would like to thank my TAC member Dr. M. Jeganmohan for his valuable discussions and suggestions, which has helped me improving my research work as well as presentation skills.

I would also like to thank all of my lab members Anant, Mahesh, Ashok, Vijayakanth, Rishabh, Santosha and Raja, who have always supported and helped me whenever required.

I thank Dr. Nirmalya Ballav lab for carrying out photocatalysis. I also thank all the instrument operators of MALDI-TOFF, NMR, HRMS, Single-crystal XRD and PXRD, who were also involved in the experiments related to my project.

I am thankful to Department of Chemistry, IISER Pune, which has provided me a wonderful opportunity for carrying out my final year project with the excellent world-class facility. And finally, I thank everyone who supported me to make this research project a success.

Contents

List of figures

Abbreviations

L^1 : $(Ph)_2PO(NH\text{-}^3Py)$

L^2: $(Ph)_2PO(NH\text{-}^4Py)$

1: $(L^1)_4Cu_4I_4$

2: $(L^2)_4Cu_4I_4$

3: $(L^2)_4Cu_4Cl_6O$

4: $(L^2)_4Cu_4Br_6O$

5: $(L^2)4Cu_4I_6O$

LE: Low-energy

HE: High-energy

^{3}CC: Cluster-centric

^{3}XMCT: Halide-to-metal charge transfer

^{3}XLCT: Halide-to-ligand charge transfer

^{3}MLCT: Metal-to-ligand charge transfer

MB: Methylene blue

Abstract

Synthesis of two pyridyl functionalized phosphorous based monodentate ligands containing P-N bonds, **L^1** & **L^2** i.e. $(Ph)_2PO(NH\text{-}^3Py)$ (^3Py = 3-pyridyl) and $(Ph)_2PO(NH\text{-}^4Py)$ (^4Py = 4-pyridyl) were carried out. These ligands were then allowed to react with copper (I) iodide, copper (I) bromide and copper (II) chloride dihydrate at room temperature as well as high temperature. Two isostructural discrete polynuclear clusters $(\mathbf{L^1})_4Cu_4I_4$ and $(\mathbf{L^2})_4Cu_4I_4$ having the $Cu_4I_4L_4$ type of self-assembly were obtained and shown to have thermochromic behavior. While, **L^2** on reacting with copper halides at different reaction conditions resulted in a rare type of $L_4Cu_4X_6O$ (X = Cl, Br, I) self-assembly containing oxide ion (O^{2-}) which do not exhibit luminescence. Further, the study of the photocatalytic activity of these complexes was done using MB (methylene blue) degradation. All the complexes obtained were able to degrade MB in the presence of H_2O_2 at room temperature. However, oxido clusters ($(\mathbf{L^2})_4Cu_4X_6O$) were found to be excellent photocatalysts. Stability of the complexes after MB degradation was confirmed by powder patterns.

Introduction

Metal-organic self-assembly is an important topic of research interest because of the facile synthesis and their ability to display unique structure driven properties.[1] While, organic ligand moieties offer tunable structural features based on shape (coordination angles), size (length and bulkiness of ligand), and functionality, the inorganic part (metal centers) in such self-assemblies invoke thermal and mechanical stabilities and afford interesting optical, magnetic or electronic properties.[2] Several reports suggest that the ligand scaffolds containing P(V) moieties can specifically afford a rigid or flexible backbone and support multimetallic assemblies in diverse structural architectures depending upon the substituents at its periphery.[3] So P(V) centered ligand motifs, viz. Phosphonate monoesters, phosphine- carboxylates, phosphine oxides, phosphonium salts, and phosphoramides have received recent attention as they can provide a flexible or rigid ligand platform around the central phosphorous with multiple coordinating sites.

Our group has been involved in synthesizing dipodal and tripodal phosphoramide ligands exhibiting various properties.[3] One of the ligands based on tripodal phosphoramide backbone, containing an electron rich aminoquinoline (AQ) chromophore, $(NHAQ)_3PO$ was shown to exhibit concentration-dependent turn on fluorescence towards picric acid.[4] This molecule shows turn on response at low concentration towards picric acid in both aqueous and non-aqueous media. At higher concentration of picric acid, luminescence quenching of the ligand takes place due to the presence of strong hydrogen bonding and π-π interactions. Application of this molecule can be found in sensing hazardous nitro explosive picric acid sensing.

Transition-metal complexes exhibiting luminescent properties have been receiving immense attention because of their various applications in detectors, chemical sensors, biological labeling and optoelectronic devices.[5] Polynuclear complexes of Pt(II), Au(I) and Cu(I) ions exhibiting external stimuli driven various photophysical properties have been reported in the literature.[6] Thus, they show properties such as thermochromism, mechanochromism, vapochromism and acidochromism in response to temperature, mechanical grinding, solvent vapor, and pH respectively.[7] Applications of such materials

can be found in temperature sensors, pressure sensors, damage detectors, etc.[8] Polynuclear clusters with copper halides and organic linkers are an interesting area of research not only because of their rigid structure but also for their rich photophysical properties. In particular, copper(I) iodide complexes have been intensively studied for their excellent luminescence behavior. For example, the cubane-type cluster $Cu_4I_4(Py)_4$ (Py = pyridyl) is very well studied in this class.[9] Interestingly, the thermochromic luminescence observed in this cluster originates from two types of bands called low energy (LE) band and high energy (HE) band (shown in figure 1a).[9, 10]

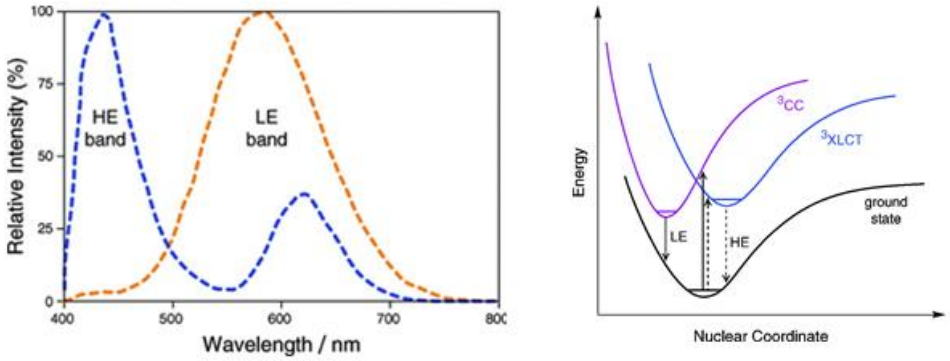

Figure 1: (a) Emission spectrum of $Cu_4I_4(Py)_4$ at 298 K (orange line) and at 77 K (blue line) (b) Simplified potential energy surface for cluster $Cu_4I_4(Py)_4$. (Taken from reference 10)

Luminescence at room temperature is dominated by low energy (LE) cluster-centred (^{3}CC) triplet emission which is due to a combination of halide-to-metal charge transfer (^{3}XMCT) and metal d → s, p transition (shown in figure 1b).[9, 10] At low temperature (77K), this band becomes weak and high energy (HE) band attributing to a triplet halide-to-ligand charge transfer (^{3}XLCT) and metal-to-ligand (^{3}MLCT) transitions are dominated.

Copper iodide clusters exhibiting rich luminescence behavior due to metallophilic interactions are an interesting class. Most commonly known copper iodide cluster exhibiting luminescence thermochromism is the cubane-type $Cu_4I_4L_4$ (L = ligand) in which there is a shift of emission wavelength with temperature due to Cu-Cu interactions.[11, 12] Various isomers of cubane having the same formula as $Cu_4I_4L_4$ exist with different geometries. Different photoluminescence behavior of these isomers compared to cubane-type complexes is interesting. These copper iodide based clusters are also found to exhibit mechanochromic luminescence in which there is a shift in the emission

wavelength in response to external mechanical force. Generally, it is seen that in a solid-state material, luminescence is dependent on the molecular structure and the packing mode of the molecule. Thus, on mechanical grinding, there are modifications in the intermolecular interactions which change the energy states of emission.[13] Cubane based copper iodide clusters having formula $Cu_4I_4L_4$ were also a family exhibiting the change of the luminescence behavior upon grinding.[14] Thus, these compounds are rare examples exhibiting both luminescence mechanochromism and thermochromism which can be used in the development of multifunctional sensing systems.

Copper iodide clusters can be obtained in different structures such as discrete clusters, cages and sometimes in MOFs and are shown to have stimuli-responsive different emissions which can be derived from their triplet state.[15] Copper iodide based MOF materials are an interesting class of compounds because of their rigid framework and their photophysical properties. For example, two isostructural hexameric copper iodide MOFs, $\{[MeSi(3Py)_3]_6(Cu_6I_6)\}_n$ (A) and $\{[MeSi(3Qy)_3]_6(Cu_6I_6)\}_n$ (B) exhibiting a reversible order of photophysical behavior have been reported.[16] The MOF A shows usual thermochromic luminescence associated with above mentioned $Cu_4I_4(Py)_4$ clusters while B shows ^{3}XLCT/^{3}MLCT emission due to the Cu_6I_6 cluster core at both 298 and 77 K.

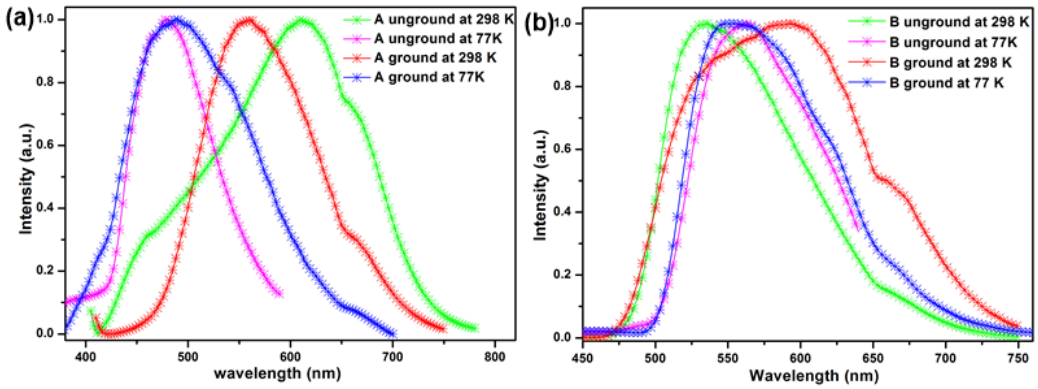

Figure 2: Solid-state photoluminescence spectra of (a) $\{[MeSi(3Py)_3]_6(Cu_6I_6)\}_n$ and (b) $\{[MeSi(3Qy)_3]_6(Cu_6I_6)\}_n$ in unground and ground states at 298 and 77 K.

These MOFs were also shown to have mechanochromic luminescence with blue-shifted HE emission and red-shifted LE emission for A and B respectively upon mechanical grinding has been observed. Solid-state photoluminescence spectra of

{[MeSi(3Py)$_3$]$_6$(Cu_6I_6)}$_n$ and {[MeSi(3Qy)$_3$]$_6$(Cu_6I_6)}$_n$ in unground and ground states at 298 and 77 K are shown in figure 2a and 2b respectively.

Despite the increasing number of reports on photophysical properties (especially thermochromism) of copper (I) iodide complexes, the unpredictable nature of the emission wavelengths, the direction of shift and change of color makes them an interesting family of compounds for photophysical studies. Also, there is only one report where copper iodide based clusters used as photocatalysts such as the one reported for the MB degradation.[17] Based on our previous results on the pyridyl functionalized tripodal phosphoramide ligands and their 2D-CuI based coordination polymers,[3f] we were interested in looking at monofunctional phosphoramide motifs as ligands for discrete CuI clusters. In this effort, we have synthesized two phosphorous based pyridyl functionalized monodentate ligands containing P-N bonds and reacted them with copper (I) iodide to study their stimuli-responsive photophysical behavior. This resulted in two discrete conventional $Cu_4I_4L_4$ (L = **L^1** & **L^2**) clusters that exhibit thermochromic luminescence behaviour. The ligands were also allowed to react with other halides such as copper (I) bromide and copper (II) chloride dihydrate which resulted in a rare type of self-assembly of polynuclear copper halide (halide = I, Br, Cl) cluster containing oxide ion (O^{2-}) having $L_4Cu_4X_6O$ (X = Cl, Br, I) type endohedral clusters with the synthesized ligand **L^2**. This is rare type of self-assembly with copper halides of oxido clusters, where luminescence is quenched unlike luminescence observed in the conventional $Cu_4I_4L_4$ (L = **L^1** & **L^2**) type of clusters. Further, the photocatalytic activity of these complexes was studied by methylene blue degradation experiment in the presence of H_2O_2.[17] All of the synthesized complexes were shown to have very good photocatalytic activity and were able to degrade MB in 30 minutes as observed by the UV-Vis spectra taken at different time intervals. However, the synthesized oxido clusters ($L_4Cu_4X_6O$) acts as excellent catalysts wherein an almost complete degradation of MB was observed. Also, the stability of these complexes after MB degradation was confirmed by the PXRD experiments. Applications of such photocatalysts can be found in the treatment of dye wastewater to degrade dye (specifically MB) before disposing it into water streams.

Methodology

General remarks

All reactions were performed under a dry nitrogen atmosphere in standard Schlenk glassware. 3-Aminopyridine, 4-Aminopyridyne, Ph_2POCl, triethylamine, CuI, CuBr, and $CuCl_2.2H_2O$ were purchased from Sigma-Aldrich and used as received. The solvent DCM was dried using distillation tube. Methylene blue and H_2O_2 were purchased from Sigma-Aldrich and were used as received. NMR spectra were recorded on a Jeol 400 MHz spectrometer (^1H NMR: 400.13 MHz; $^{13}C\{^1H\}$NMR, 100.62 MHz; $^{31}P\{^1H\}$ NMR, 161.97 MHz) at room temperature using SiMe4 (^1H, ^{13}C) and H_3PO_4 (^{31}P) as external standards. The MALDI-TOF spectra were obtained from Applied Biosystem MALDI-TOF/TOF spectrometer. The powder X-ray diffraction (PXRD) data were obtained from a Bruker-D8 Advance diffractometer. The absorption studies were done by a PerkinElmer Lambda 45 UV−visible spectrophotometer. Emission spectra were recorded on a SPEX Fluorolog HORIBA JOBIN VYON spectrophotometer with a double grating 0.22 m SPEX 1680 monochromator and a 450 W Xe lamp as the excitation source. Photocatalysis was done using 200W daylight lamp.

Synthesis

L^1: 3-amino pyridine (0.5gm, 5.3 mmol, 1 eq.) was dissolved in 30 ml of dry dichloromethane under an inert atmosphere. To this solution triethylamine (0.85ml, 6 mmol, and 1.1 eq.) was added. After stirring for 15 min, Ph_2POCl (1ml, 5.3 mmol, 1eq.) was added dropwise to the mixture at 0˚C. The reaction mixture was further allowed to stir for 6 h at room temperature. A saturated aqueous solution of $NaHCO_3$ (10 ml) was added to the mixture and stirred for 15 min, and then the layers were separated. The aqueous layer was extracted 2-3 times with CH_2Cl_2. The combined organic layers were dried using Na_2SO_4 and then concentrated. The resulting phosphoramide compound was found to have 71 % yield. **L^1** was characterized by MALDI-TOF, HRMS, ^1H, ^{13}C and ^{31}P NMR. ^1H NMR, ^{13}C NMR, MALDI-TOF, HRMS, ^{31}P NMR confirms the formation of **L^1** in

pure form which is discussed in result and discussion part. Crystal of **L^1** was obtained by slow evaporation of methanol in which **L^1** was dissolved. Unit cell parameters: a= 26.00, b= 3.965, c= 20.99, α=90, monoclinic C 2/c, Volume 3001.19 $Å^3$.

^{1}H NMR (400.13 MHz, $CDCl_3$): δ = 8.3 (1H), 8.0 (1H), 7.8-7.9 (m, 4H), 7.35-7.55 (m, 6H), 6.95 (1H), 6.8 (1H) ppm. ^{13}C (100.62 MHz, $CDCl_3$): δ - 142.57, 140.44, 137.82, 132.46, 132.01, 130.68, 128.83, 125.30, 123.56 ppm. ^{31}P NMR (161.97 MHz, $CDCl_3$): δ = 19.26 ppm. MALDI-TOF m/z = 295 $[M+H]^+$, 317 $[M+Na]^+$, 333 $[M+K]^+$.

L^2: Synthesis of **L^2** was carried out by following the reported procedure.[18] 4-amino pyridine (0.5gm, 5.3 mmol, 1 eq.) was dissolved in 30 ml of dry dichloromethane under an inert atmosphere. To this solution, triethylamine (0.85ml, 6 mmol, and 1.1 eq.) was added. After stirring for 15 min, Ph_2POCl (1ml, 5.3 mmol, 1eq.) was added dropwise to the mixture at 0˚C. The reaction mixture was further allowed to stir for 6 h at room temperature. A saturated aqueous solution of $NaHCO_3$ (10 ml) was added to the mixture and stirred for 15 min, and then the layers were separated. The aqueous layer was extracted 2-3 times with CH_2Cl_2. The combined organic layers were dried using Na_2SO_4 and then concentrated. The resulting phosphoramide compound was found to have 82 % yield. **L^2** was also characterized by MALDI-TOF, HRMS, ^{1}H, ^{13}C and ^{31}P NMR. ^{1}H NMR, ^{13}C NMR, MALDI-TOF, HRMS, ^{31}P NMR confirms the formation of **L^2** in pure form which is discussed in result and discussion part.

^{1}H NMR (400.13 MHz, $CDCl_3$): δ = 8.1 (2H), 7.75-7.85 (m, 4H), 7.35-7.55 (m, 6H), 6.85 (2H) ppm. ^{13}C (100.62 MHz, $CDCl_3$): δ - 149.86, 148.79, 132.71, 131.94, 131.84, 129.08, 113.16 ppm. ^{31}P NMR (161.97 MHz, $CDCl_3$): δ = 20.05 ppm. MALDI-TOF m/z = 295 $[M+H]^+$, 317 $[M+Na]^+$, 333 $[M+K]^+$.

1: To a solution of **L^1** (14.7 mg, 0.05 mmol) in DCM (2 ml) was added a solution of CuI (9.5 mg , 0.05 mmol) in acetonitrile (1 ml) which was then stirred for 30 min. to get brown colored precipitate which was then heated at 120 °C under the solvothermal condition for 36 h. The resultant solution was slowly cooled to room temperature for 15 hrs to yield small yellow-colored crystals of **1**. The yield of the crystal **1** was around 2 mg. Unit cell

parameters: a=15.42, b=18.159, c=28.072, α=90, β= 93.84, γ=90, monoclinic C 2/c, Volume = 7842.98 $Å^3$.

2: Above the solution of **L^2** (7.4 mg, 0.025 mmol) in DCM (2 ml) taken in layering tube was slowly added a layer of clean DCM (0.5 ml) above which a layer of a solution of CuI (4.8 mg, 0.025 mmol) in acetonitrile (1 ml) was added. The resulting system was packed and kept at ambient temperature for slow diffusion without disturbing it. After one week yellowish brown colored crystals of **2** were obtained. The yield of the crystal **1** was around 2 mg. Unit cell parameters: a= 22.969, b= 22.969, c= 15.2023, α=90, β= 90, γ=90, tetragonal I 4_1/a, Volume = 8020.07$Å^3$.

3: Above the solution of **L^2** (7.4 mg, 0.025 mmol) in $CHCl_3$ (2 ml) taken in layering tube was slowly added a layer of clean $CHCl_3$ (0.5 ml) above which a layer of a solution of $CuCl_2.2H_2O$ (4.3 mg, 0.025 mmol) in acetonitrile (1 ml) was added. The resulting system was packed and kept at ambient temperature for slow diffusion without disturbing it. After one week dark brownish yellow colored crystals of **3** were obtained. The yield of the crystal **3** was around 1 mg. Unit cell parameters: a= 22.262, b= 22.262, c= 15.841, α=90, β= 90, γ=90, tetragonal I 4_1/a, Volume = 8571.31 $Å^3$.

4: Above the solution of **L^2** (7.4 mg, 0.025 mmol) in $CHCl_3$ (2 ml) taken in layering tube was slowly added a layer of clean $CHCl_3$ (0.5 ml) above which a layer of a solution of CuBr (3.6 mg, 0.025 mmol) in acetonitrile (1 ml) was added. The resulting system was packed and kept at ambient temperature for slow diffusion without disturbing it. After one week intense brown colored crystals of **4** were obtained. The yield of the crystal **3** was around 1.5 mg. Unit cell parameters: a= 24.081, b= 24.081, c= 14.967, α=90, β= 90, γ=90, tetragonal I 4_1/a, Volume = 8679.43 $Å^3$.

5: To a solution of **L^2** (14.7 mg, 0.05 mmol) in DCM (2 ml) was added a solution of CuI (9.5 mg , 0.05 mmol) in acetonitrile (1 ml) which was then stirred for 30 min. to get white colored precipitate which was then heated at 120 °C under the solvothermal condition for 36 h. The resultant solution was slowly cooled to room temperature for 15 hrs to yield brownish yellow colored crystals of **5**. The yield of the crystal **3** was around 1.5 mg. Unit cell parameters: a= 23.922, b= 23.922, c= 15.527, α=90, β= 90, γ=90, tetragonal I 4_1/a, Volume = 8885.38 $Å^3$.

Results and Discussion

The ligands **L¹** and **L²** were synthesized from the respective reaction 3-bromopyridine and 4-bromopyridine with Ph_2POCl in the presence of triethylamine in refluxing DCM. The ligands were characterized by mass spectroscopy, ^{31}P, ^{1}H and ^{13}C NMR and crystallography in the case of **L¹**. The reaction schemes and conditions for the formation of **L¹** and **L²** are shown in figure 3 (Scheme 1).

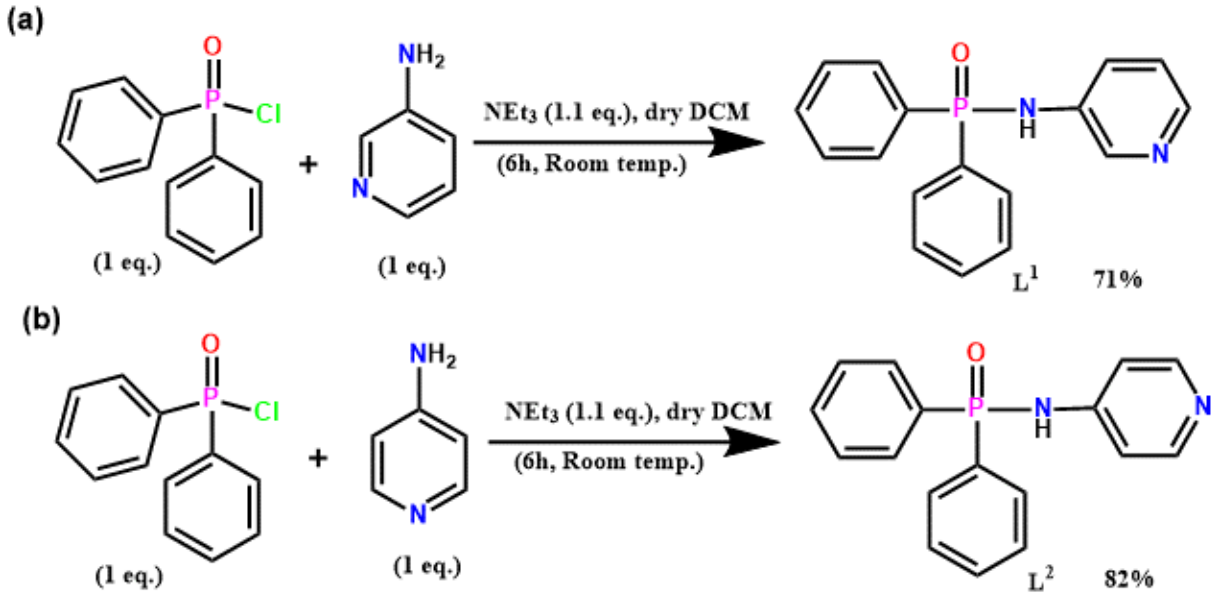

Figure 3: Reaction schemes and conditions for the formation of **L¹** and **L²**.

Characterization of L¹ and L²

To confirm the formation of **L¹** and **L²** MALDI-TOF spectra was taken which is shown in figure 4. The MALDI spectra show the peaks corresponding to the expected mass i.e. 294 for both **L¹** and **L²**. Peaks at 295, 317 and 333 correspond to $[M+H]^+$, $[M+Na]^+$ and $[M+K]^+$ respectively which clearly shows the formation of **L¹** and **L²**. In addition to MALDI-TOF, the HRMS data was also taken and is shown in figure 5.

The formation of **L¹** and **L²** was further confirmed by ^{1}H, ^{13}C, and ^{31}P (shown in figure 6, 7 and 8 respectively).

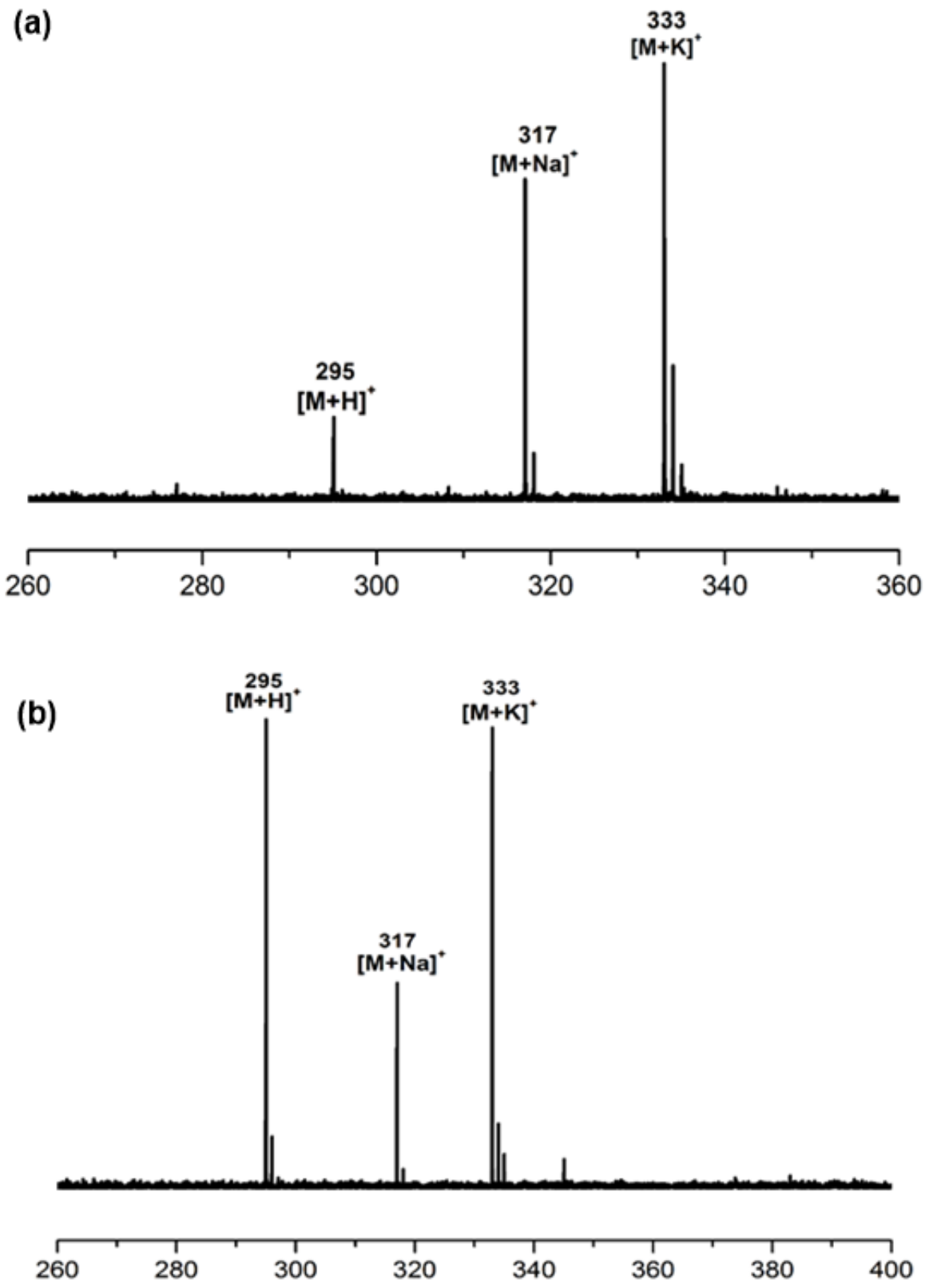

Figure 4 : MALDI-TOF spectra of (a) $\mathbf{L^1}$ and (b) $\mathbf{L^2}$.

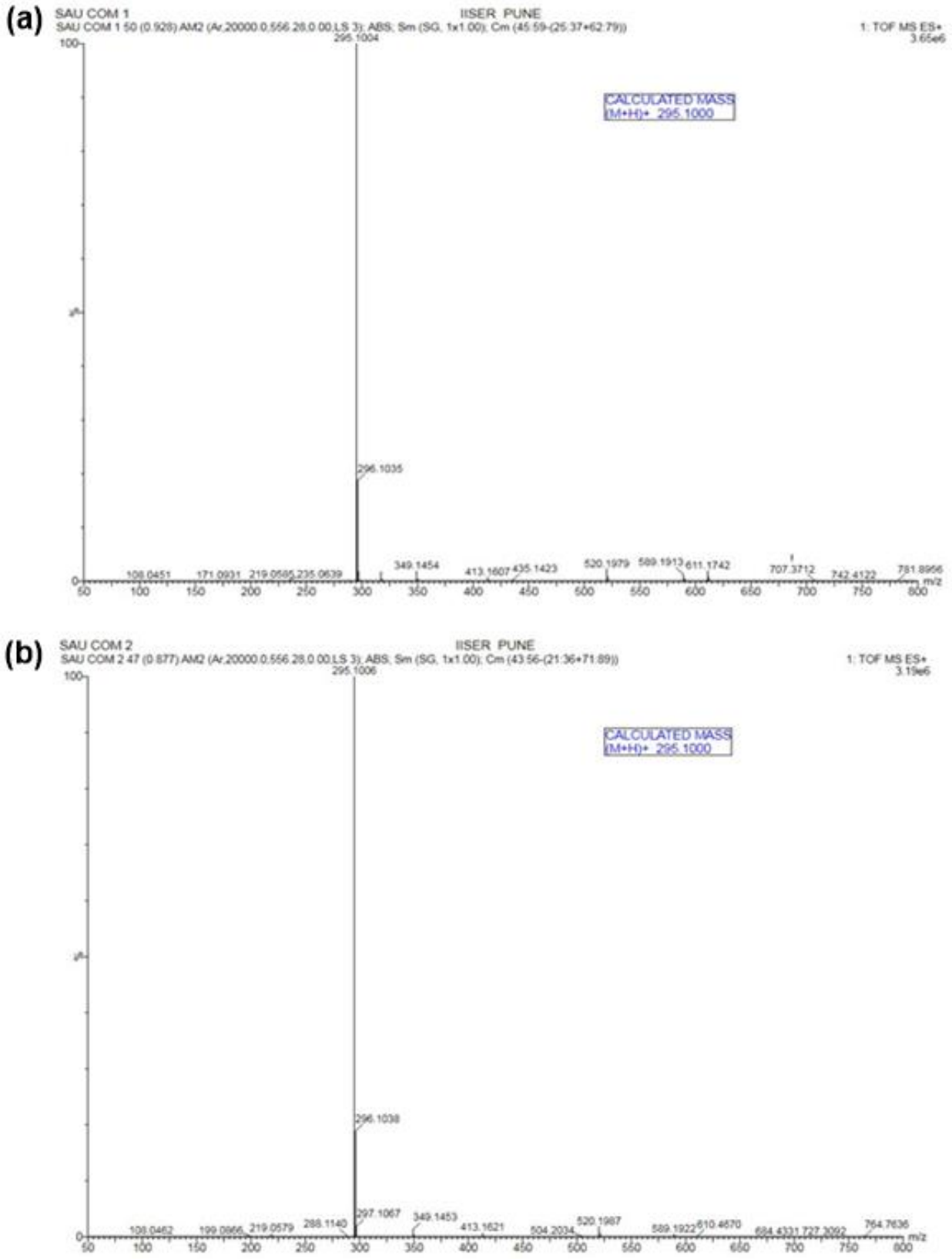

Figure 5 : HRMS spectra of (a) **L[1]** and (b) **L[2]**.

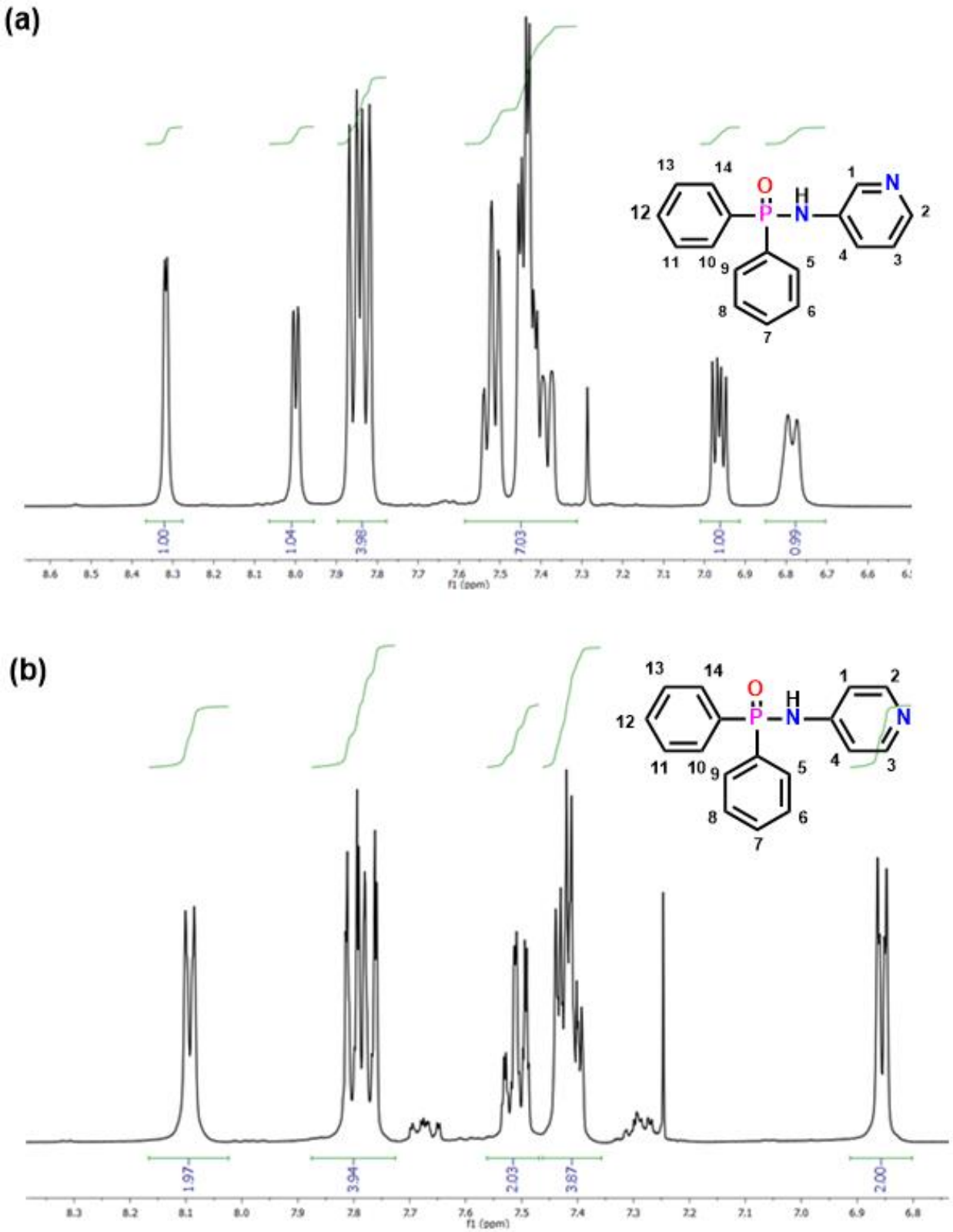

Figure 6 : ^{1}H NMR spectra of (a) $\mathbf{L^1}$ and (b) $\mathbf{L^2}$.

From the NMR spectrum of **L^1** given in figure 6a, the singlet peak at 8.3 ppm corresponds to the most deshielded proton, i.e., H^1, while the doublet at 8.0 ppm is due to H^3. The multiplet at 7.85 ppm is due to H^5, H^9, H^{10} and H^{14} protons due to their similar chemical environment. The peaks between 7.35 and 7.55 ppm (with integration 7) include one –NH proton near to P and the protons of H^6, H^7, H^8, H^{11}, H^{12}, and H^{13}. Finally, the peaks at 6.95 and 6.8 ppm correspond to H^3 and H^4 protons, respectively.

Similarly from the spectrum of **L^2** given in figure 6b, the doublet at 8.1 ppm (with integration 2) is due to the most deshielded protons i.e. H^2 and H^3. The multiplet at 7.8 ppm (with integration 4) is due to protons H^5, H^9, H^{10} and H^{14} with the similar chemical environment. The multiplet between 7.35 t and 7.5 ppm (with total integration of 6) corresponds to the protons of H^6, H^7, H^8, H^{11}, H^{12}, and H^{13}, while the doublet at 6.85 ppm is due to H^1 and H^4.

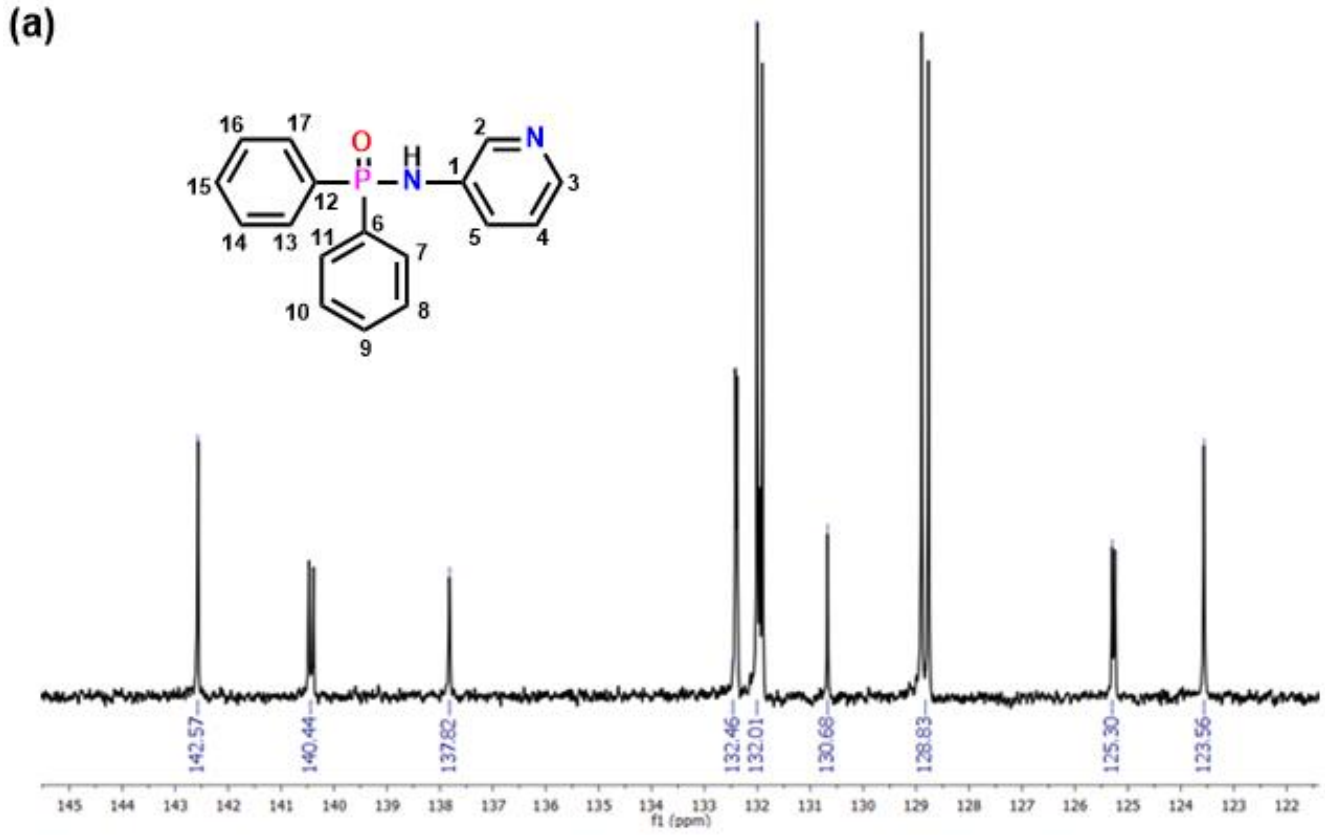

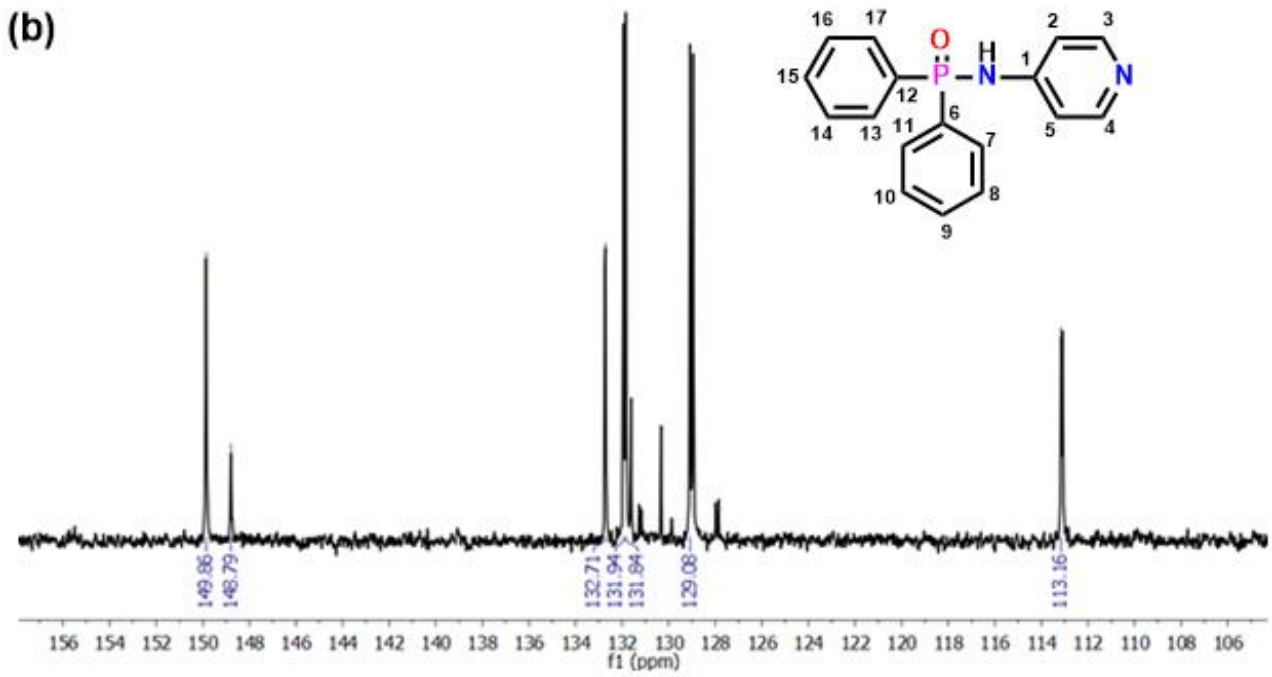

Figure 7: ^{13}C NMR spectra of (a) **L^{1}** and (b) **L^{2}**.

In the ^{13}C NMR of **L^{1}** shown in figure 7a, the peak at 143.57 ppm is most deshielded carbon which is directly attached to the nitrogen attached to phosphorous i.e. C^{1}. The peak at 140.44 and 137.82 ppm is due to C^{2} and C^{3} respectively. The peak at 132.46 ppm corresponds to C^{9} and C^{15} while the peak at 132.01 ppm corresponds to four carbons C^{8}, C^{10}, C^{14} and C^{16} having similar kind of chemical environment. The peak at 130.68 ppm corresponds to the carbons directly attached to phosphorous i.e. C^{6} and C^{12} while the peak at 128.83 ppm is due to C^{7}, C^{11}, C^{13}, and C^{17}. The peak and 125.30 and 123.56 ppm corresponds to C^{4} and C^{5} respectively.

Similarly in the ^{13}C NMR of **L^{2}** shown in figure 7b, the peak at 140.96 ppm is most deshielded carbon which is directly attached to N attached to P i.e. C^{1}. The peak at 148.79 ppm is due to the two similar carbons C^{3} and C^{4} attached to the nitrogen of aromatic ring. The peak at 132.71 ppm corresponds to C^{9} and C^{15} while the two peaks at 131.94 and 131.84 ppm are because of C^{6}, C^{12}, and C^{8}, C^{10}, C^{14} & C^{16} respectively. The peaks at 129.08 and 131.16 ppm correspond to C^{7}, C^{11}, C^{13} & C^{17} and C^{2} &C^{5} respectively.

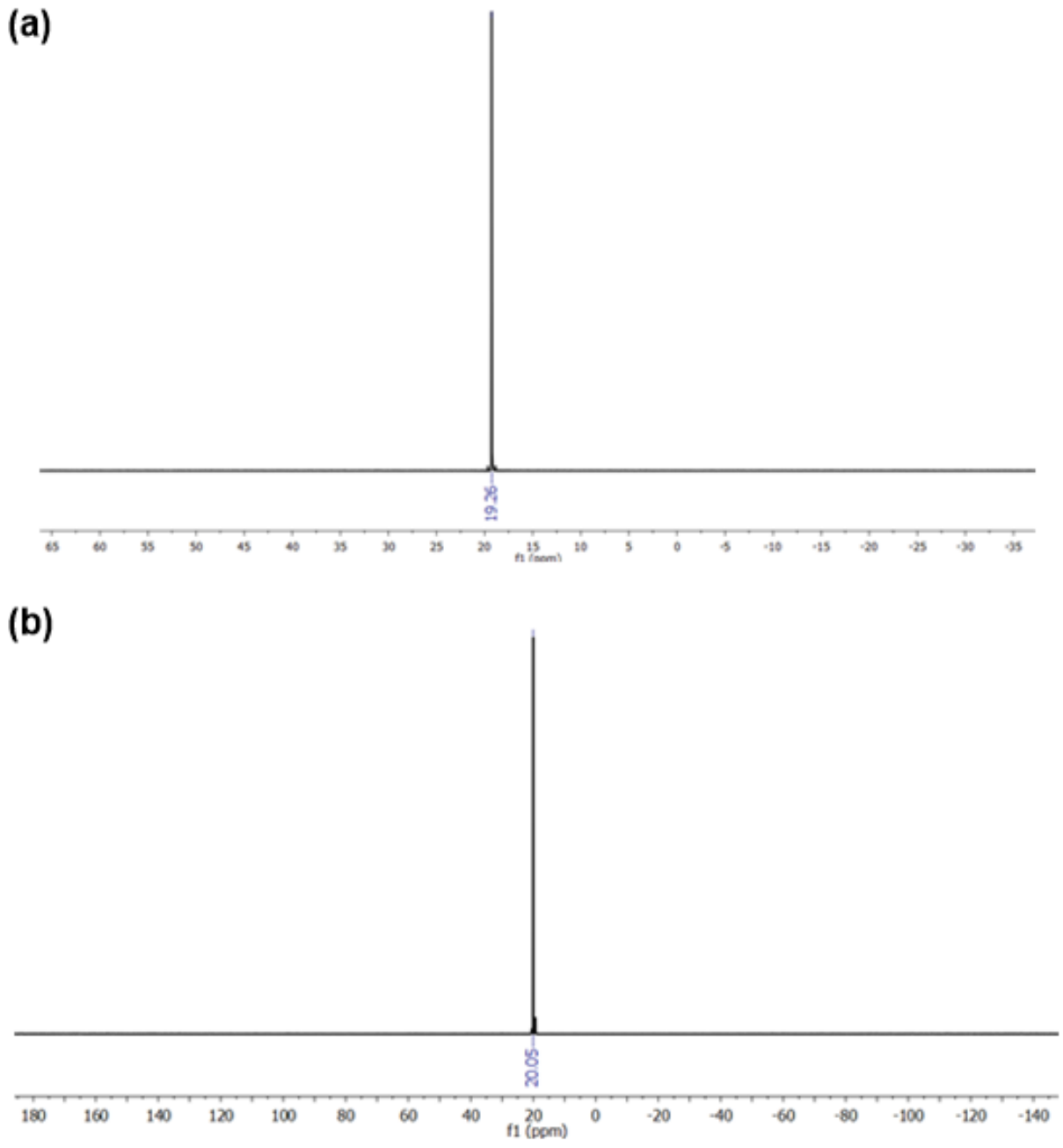

Figure 8: ^{31}P NMR spectra of (a) **L^{1}** and (b) **L^{2}**.

The ^{31}P-NMR spectra of **L^{1}** and **L^{2}** show a single peak at δ =19.26 and 20.05 ppm respectively confirming the formation of ligands in their pure form hence no other phosphorous impurity. Hence, all the characterization techniques mentioned above clearly show the formation of ligands **L^{1}** and **L^{2}** in their pure form.

Reaction of L^1 and L^2 with Copper halides

L^1 and **L^2** were dissolved in DCM and were added to copper iodide solution in acetonitrile which was then stirred for half an hour to get a brown and white colored precipitates respectively which were then kept at 120 °C under solvothermal conditions to obtain clusters **1** and **5** respectively. While crystals of the cluster **2**, **3** and **4** were obtained by the reaction of 1 equivalent CuI, $CuCl_2.2H_2O$ and CuBr with **L^2** by layering method of solvent diffusion at room temperature, in which **L^2** was dissolved in DCM and added to the empty layering tube above which neat layer of DCM was added and then the respective CuI, $CuCl_2.2H_2O$ and CuBr solution in acetonitrile was added slowly as the top layer. The system was left for slow diffusion at room temperature and the crystals of **2**, **3** and **4** were obtained.

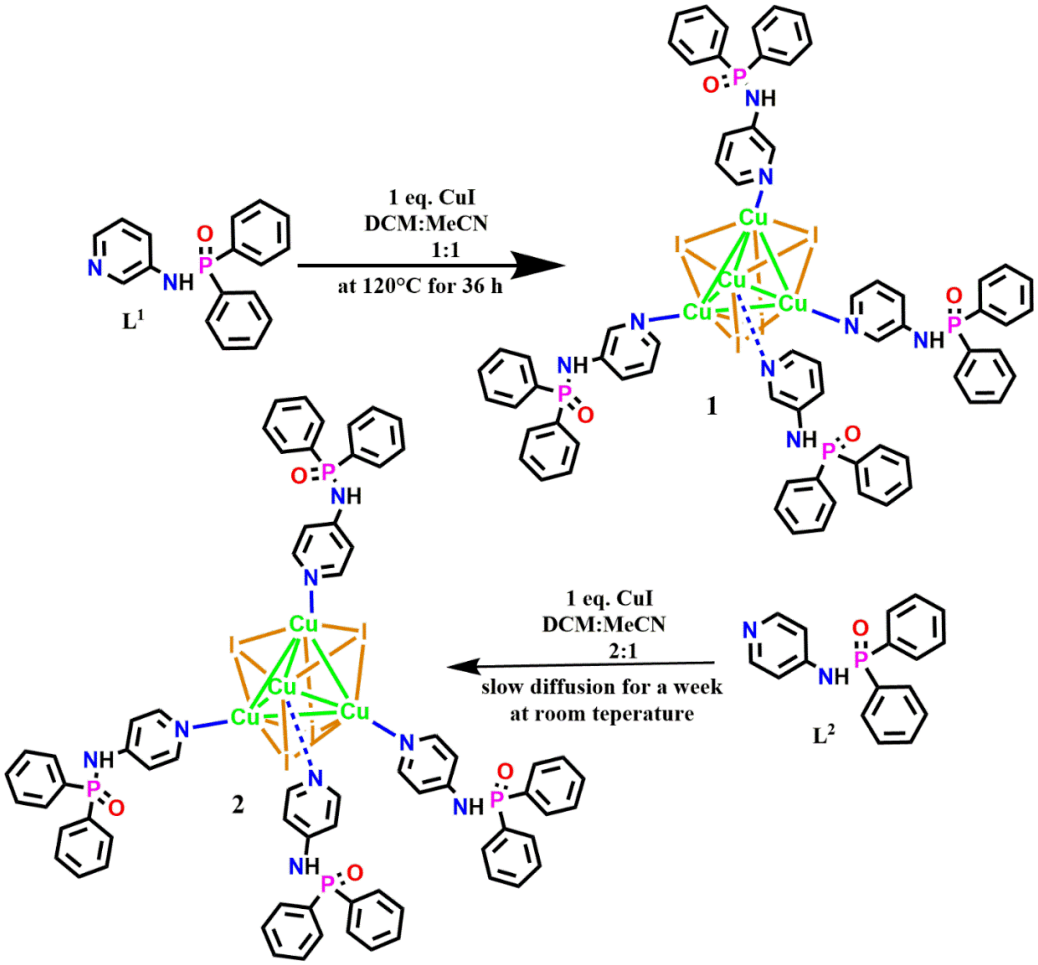

Figure 9: Reaction schemes and conditions for the formation of **1** and **2**.

1 and **2** were obtained as discrete isostructural Cu_4I_4 clusters which are shown to have thermochromic luminescence behavior while **3**, **4** and **5** were obtained as discrete isostructural Cu_4X_6O (X = Cl, Br & I) clusters and there is no luminescence shown by them. Reaction scheme and conditions for the formation of **1** & **2** are shown in figure 9 (scheme 2) and reaction scheme and conditions for the formation of **2**, **3** & **5** is shown in figure 10 (scheme 3).

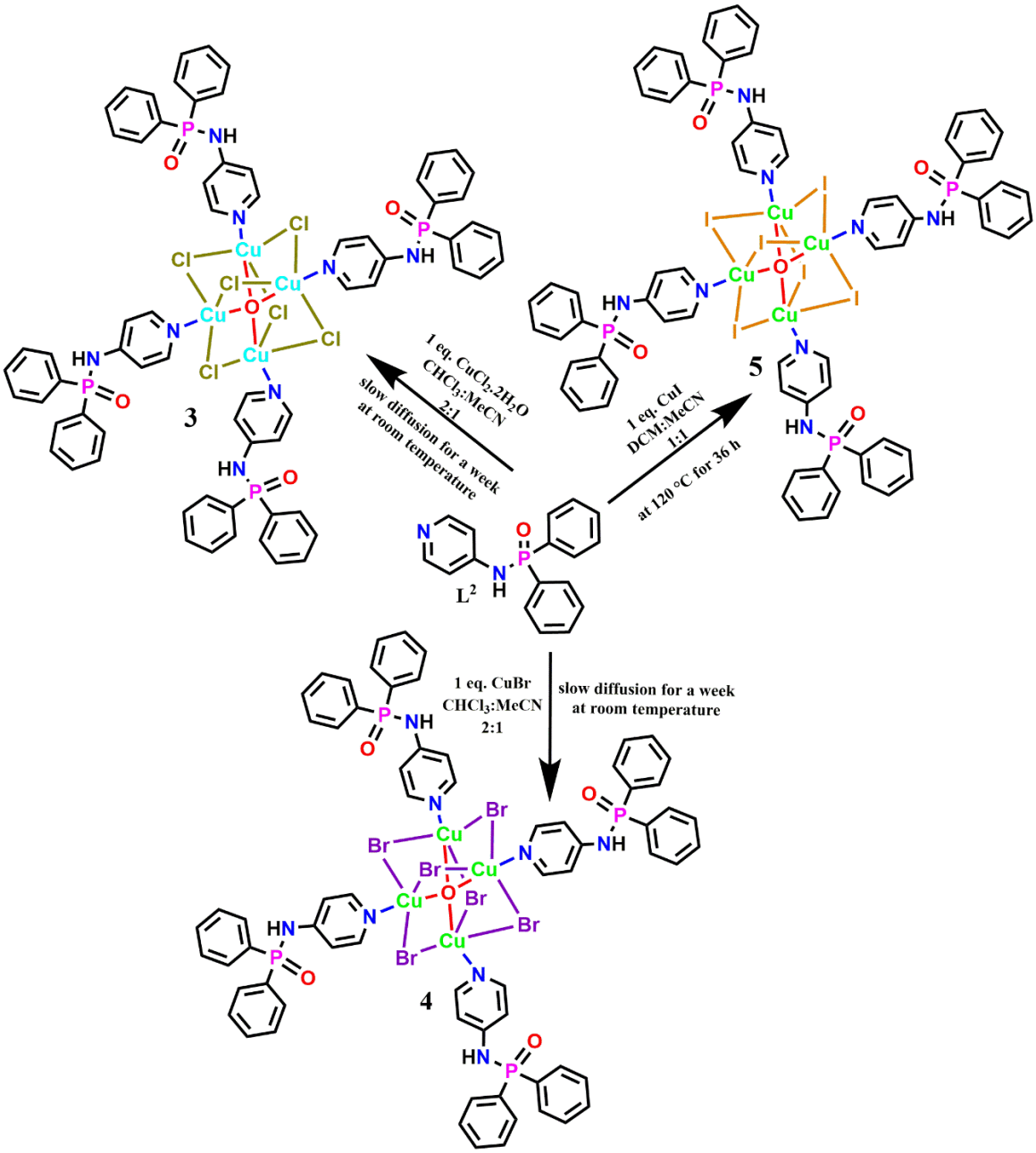

Figure 10: Reaction schemes and conditions for the formation of **3**, **4** and **5**.

Crystal structures

Reflections were collected on a Bruker Smart Apex Duo diffractometer at 100 K using Mo Kα radiation (λ = 0.71073 Å). Structures were refined by full-matrix least squares against F2 using all data (SHELX).

The molecular structure of **1** was solved in monoclinic space group C 2/c. Asymmetric unit of **1** consists of two Cu(I) ions, two I^- ions and two units of ligand (shown in figure 11b). The molecular core of **1** consists of a tetrameric unit Cu_4I_4 (shown in figure 11a), in which each I^- acts as a μ3-bridging unit. The Cu(I) ions are located in a tetrahedral coordination consisting of three I^- contacts and one pyridyl N-donor in contact. The unit cell parameters for the crystal **1** are a=15.42, b=18.159, c=28.072, α=90, β= 93.84, γ=90 and the volume of the unit cell is found to be 7842.98 $Å^3$.

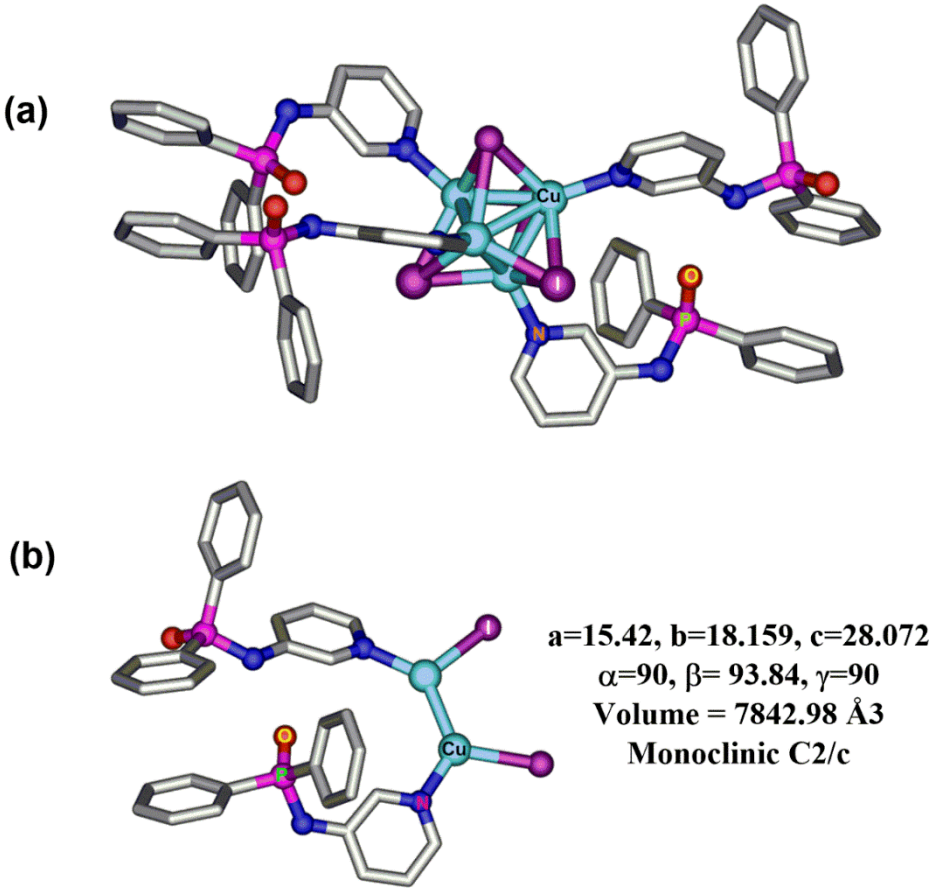

Figure 11: Crystal structure of **1** (a) showing the $(\mathbf{L^1})_4Cu_4I_4$ cluster and (b) its asymmetric unit.

The molecular structure of **2** was solved in tetragonal space group I 4_1/a. Asymmetric unit of **2** consists of one Cu(I) ion, one I^- ions and one unit of ligand (shown in figure 12b). The molecular core of **2** consists of a tetrameric unit Cu_4I_4 (shown in figure 12a), in which each I^- acts as a μ3-bridging unit. The Cu(I) ions are located in a tetrahedral coordination consisting of three I^- contacts and one pyridyl N-donor in contact. The unit cell parameters for the crystal **2** are a= 22.969, b= 22.969, c= 15.2023, α=90, β= 90, γ=90 and the volume of the unit cell is found to be 8020.07$Å^3$.

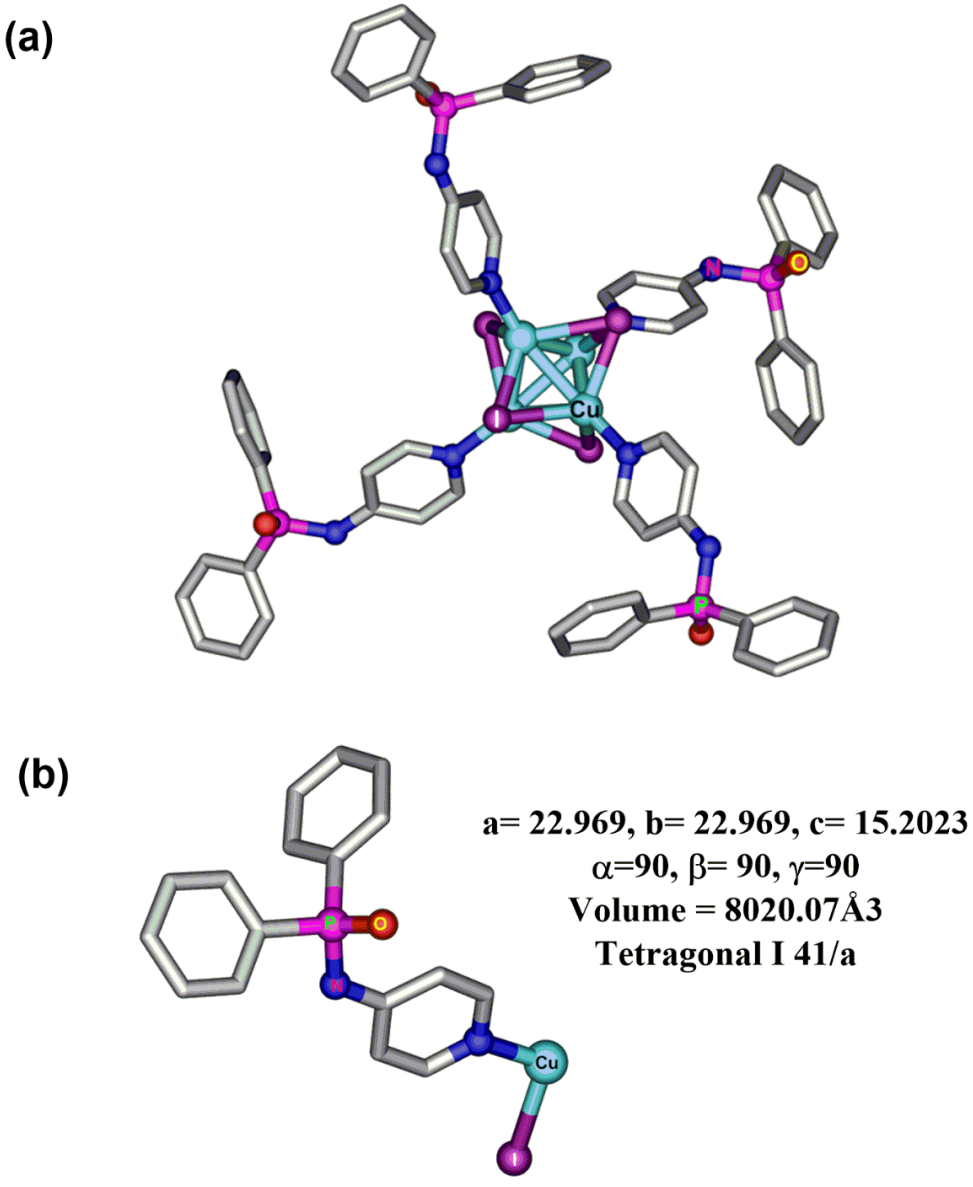

Figure 12: Crystal structure of **2** (a) showing the $(\mathbf{L^2})_4Cu_4I_4$ cluster and (b) its asymmetric unit.

L² on reacting with $CuCl_2.2H_2O$ and CuBr by slow diffusion method and with CuI at 120°C under solvothermal conditions was self-assembled as a discrete isostructural Cu_4X_6O (i.e. Cu_4I_6O, Cu_4Cl_6O & Cu_4Br_6O) type of clusters. This type of unconventional self-assembly having O^{2-} is very rare where luminescence is quenched. Corresponding crystal structure and their asymmetry unit of complexes **3**, **4** and **5** are discussed below.

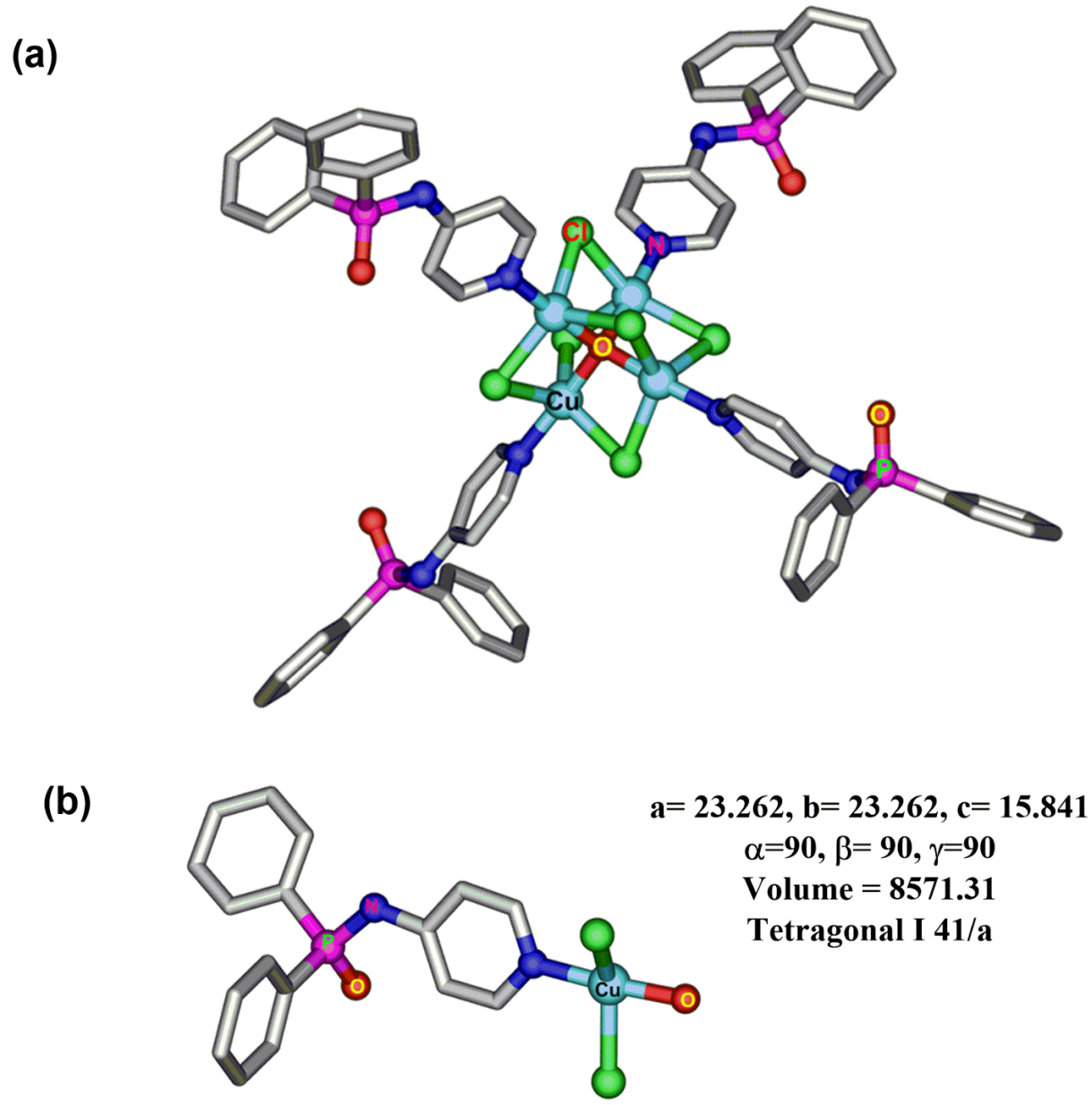

Figure 13: Crystal structure of **3** (a) showing the $(\mathbf{L^2})_4Cu_4Cl_6O$ cluster and (b) its asymmetric unit.

The molecular structure of **3** was solved in tetragonal space group I 4_1/a. The asymmetric unit of **3** consists of one Cu(II) ion, two Cl^- ions, one O^{2-} ion and one unit of ligand (shown in figure 13b). The molecular core of **3** consists of a Cu_4Cl_6O unit (shown in figure 13a), in which each Cl^- acts as a μ2-bridging unit while the O^{2-} at the center is connected to all the Cu atoms. The Cu(II) ions are located in the coordination consisting of three Cl^- contacts, one O^{2-} contact and one pyridyl N-donor in contact. The unit cell parameters for the crystal **3** are a= 22.262, b= 22.262, c= 15.841, α=90, β= 90, γ=90 and the volume of the unit cell is found to be 8571.31 $Å^3$.

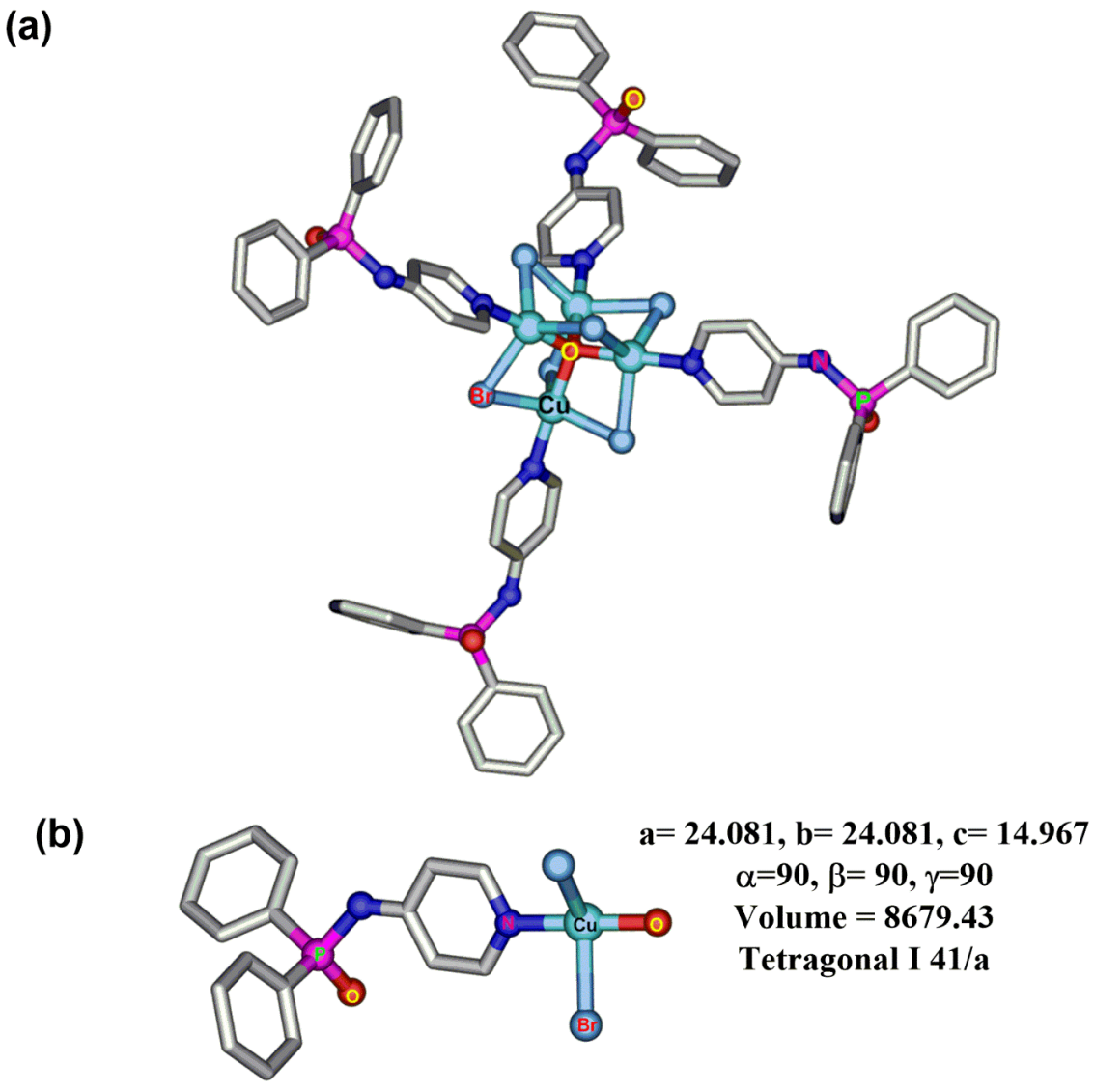

Figure 14: Crystal structure of **4** (a) showing the $(\mathbf{L^2})_4Cu_4Br_6O$ cluster and (b) its asymmetric unit.

The molecular structure of **4** was solved in tetragonal space group I 4_1/a. The asymmetric unit of **4** consists of one Cu(II) ion, two Br^- ions, one O^{2-} ion and one unit of ligand (shown in figure 14b). The molecular core of **4** consists of a Cu_4Br_6O unit (shown in figure 14a), in which each Br^- acts as a μ2-bridging unit while the O^{2-} at the center is connected to all the Cu atoms. The Cu(II) ions are located in the coordination consisting of three Br^- contacts, one O^{2-} contact and one pyridyl N-donor in contact. The unit cell parameters for the crystal **4** are a= 24.081, b= 24.081, c= 14.967, α=90, β= 90, γ=90 and the volume of the unit cell is found to be 8679.43 $Å^3$.

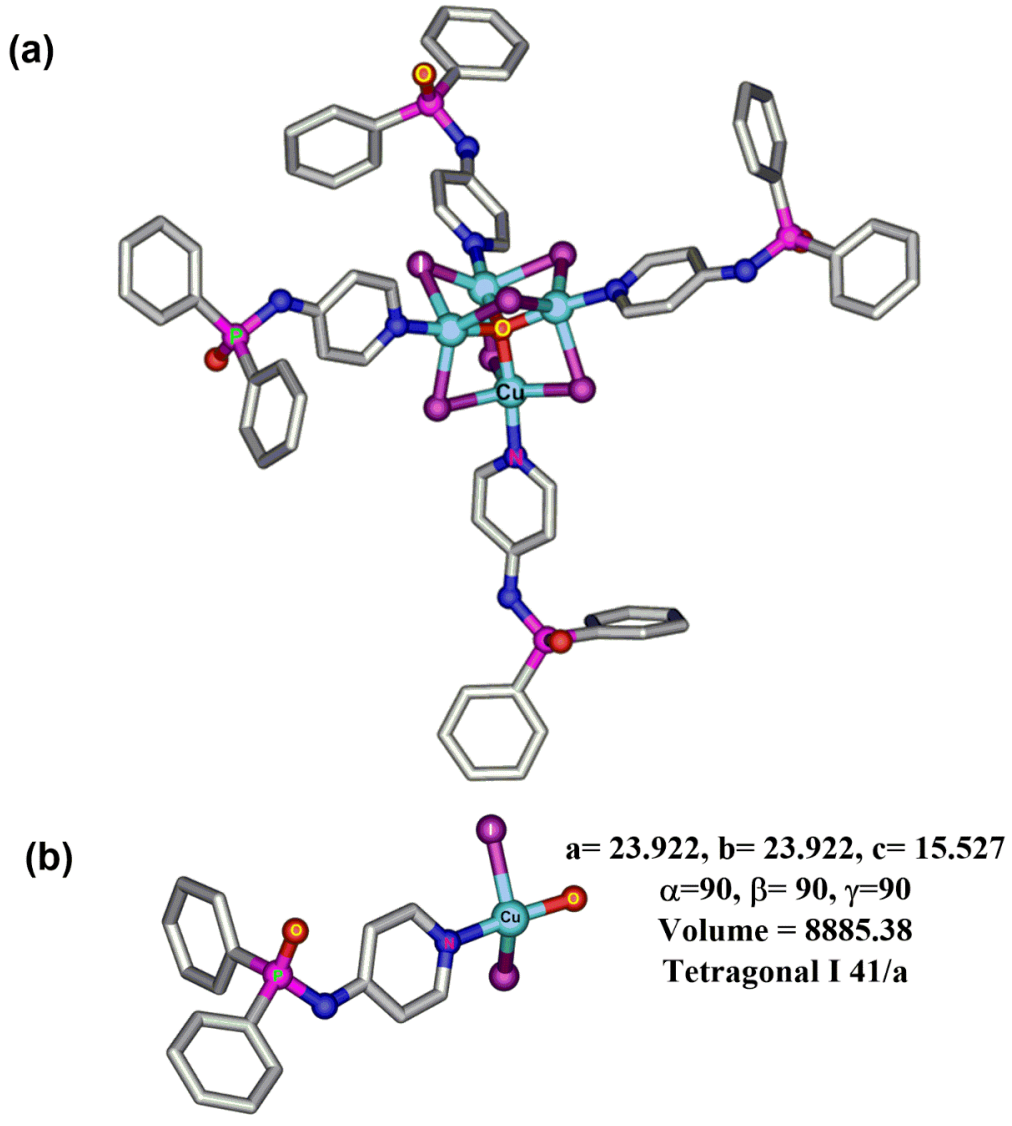

Figure 15: Crystal structure of **5 (a)** showing the $(\mathbf{L^2})_4Cu_4I_6O$ cluster and (b) its asymmetric unit.

The molecular structure of **5** was solved in tetragonal space group I $4_1/a$. The asymmetric unit of **5** consists of one Cu(II) ion, two I^- ions, one O^{2-} ion and one unit of ligand (shown in figure 15b). The molecular core of **5** consists of a Cu_4I_6O unit (shown in figure 15a), in which each I^- acts as a μ2-bridging unit while the O^{2-} at the center is connected to all the Cu atoms. The Cu(II) ions are located in the coordination consisting of three I^- contacts, one O^{2-} contact and one pyridyl N-donor in contact. The unit cell parameters for the crystal **5** are a= 23.922, b= 23.922, c= 15.527, α=90, β= 90, γ=90 and the volume of the unit cell is found to be 8885.38 $Å^3$.

L^1 was dissolved in methanol and kept in the vial at room temperature for solvent evaporation. After 2-3 days crystals of **L^1** were obtained. The molecular structure of **L^1** was solved in monoclinic space group C 2/c. The unit cell parameters for the crystal were a= 26.00, b= 3.965, c= 20.99, α=90, β= 112.73, γ=90 and the volume of the unit cell was found to be 3001.19 $Å^3$. The crystal structure of **L^1** is shown in figure 16.

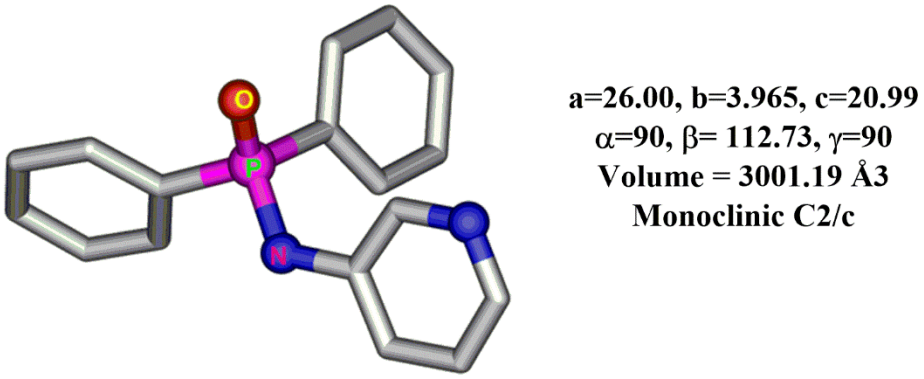

Figure 16: Crystal structure and unit cell parameters of **L^1**.

Photophysical properties

L^1 was dissolved in DCM and was added to copper iodide solution in acetonitrile which was then stirred for half an hour to get a brown colored precipitate of copper iodide complex **1**. This precipitate was seen under UV (365 nm) and was shown to have orange color luminescence at room temperature. On decreasing the temperature to 77 K using liquid nitrogen, the precipitate was shown to emit reddish pink color (shown in figure 17a).

Similarly, **L²** was dissolved in DCM and was added to copper iodide solution in acetonitrile which was then stirred for half an hour to get a pale white colored precipitate of copper iodide complex **2**. This precipitate was seen under UV (365 nm) and was shown to have orange color photoluminescence at room temperature. On decreasing the temperature to 77 K using liquid nitrogen, the precipitate was shown to emit bright reddish orange color (shown in figure 17b). This property of emitting photoluminescence of different color at a different temperature is called thermochromism. Thus obtained copper iodide complex **1** & **2** were shown to have thermochromic luminescence property under UV (365 nm).

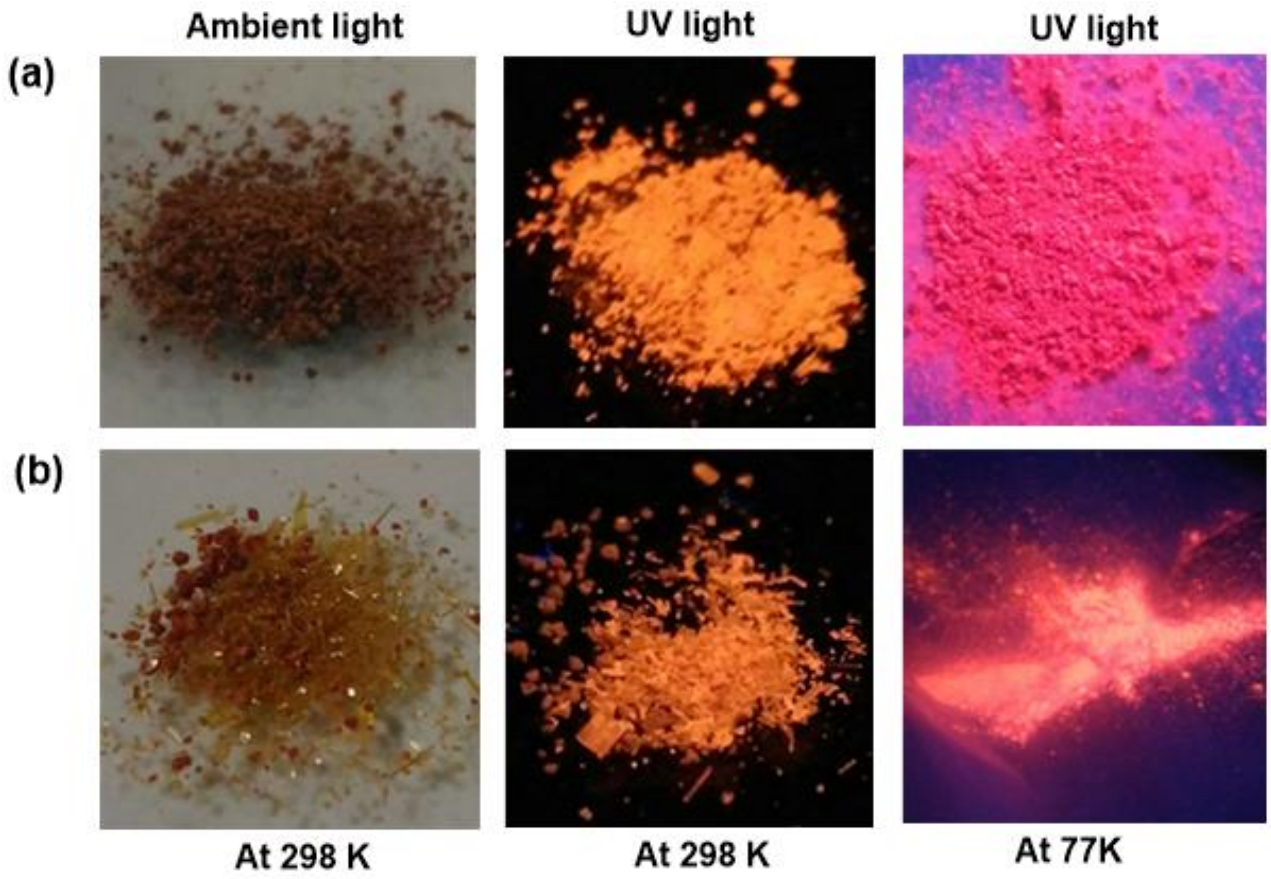

Figure 17: Solid-state emission colors of various (a) Complex **1** and (b) Complex **2** under ambient light and UV lamp (irradiated at 365 nm).

The original emission color of **1** and **2** at can be recovered back within few minutes on gradually warming the sample to room temperature suggesting a completely reversible thermochromism in both of them. To understand this phenomenon, the excitation (shown in figure 18) and emission spectra (figure 19) of **1** and **2** were recorded in the solid state.

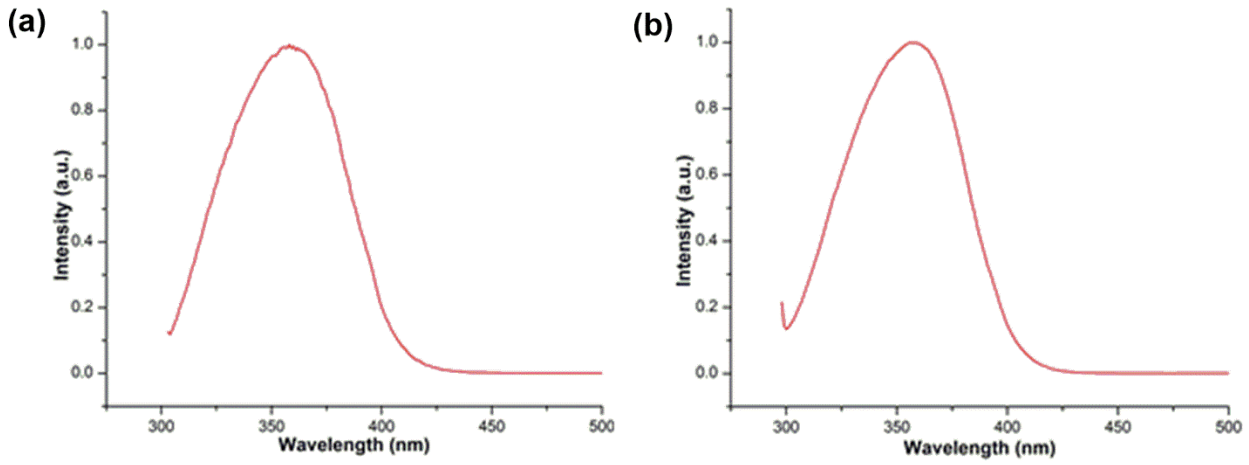

Figure 18 : Solid-state excitation spectra of (a) complex **1** and (b) complex **2** at room temperature.

At 298 K, the emission spectrum of **1** shows an intense low-energy (LE) emission band centered at 600 nm (λ_{ex} = 358 nm, figure 19a) which is in agreement with orange colored emission observed at room temperature. In addition, there is a very weak high-energy (HE) band at around 440 nm. However, at 77 K this HE band was prominently visible, and the LE band was slightly red-shifted to 628 nm. It can be seen that the luminescence at room temperature is dominated by a low energy (LE) band which can be attributed to the cluster-centric ^{3}CC transition comprising of halide to metal charge transfer (^{3}XMCT) and Cu d → s, p transition. At low temperature (77K), the high energy (HE) band starts appearing which is due to a mixture of halide to ligand charge transfer (^{3}XLCT) and metal to ligand charge transfer (^{3}MLCT) transitions. Both these transitions were well established with traditional $Cu_4I_4Py_4$ type clusters. At further lower temperature (maybe 4 K), it is expected that the high energy (HE) band would become more intense, and the intensity of low energy (LE) band would go down.

Similarly, the emission spectrum of **2** displays an intense broad emission band (LE) centered at 592 nm (λ_{ex} = 356 nm, figure 19a) with a very weak HE band around 430 nm at 298 K. The LE band corresponds to the orange colored emission due to ^{3}CC transitions. The emission spectrum of **2** at 77 K could not be taken due to due to some problem in the fluorescence instrument and will be taken in future when the problem is fixed. But it is expected that the trend would be similar as seen in the case of **1** and the HE band

would appear at 77 K which would further become more intense and the intensity of low energy (LE) band would go down at lower temperature (around 4 K).

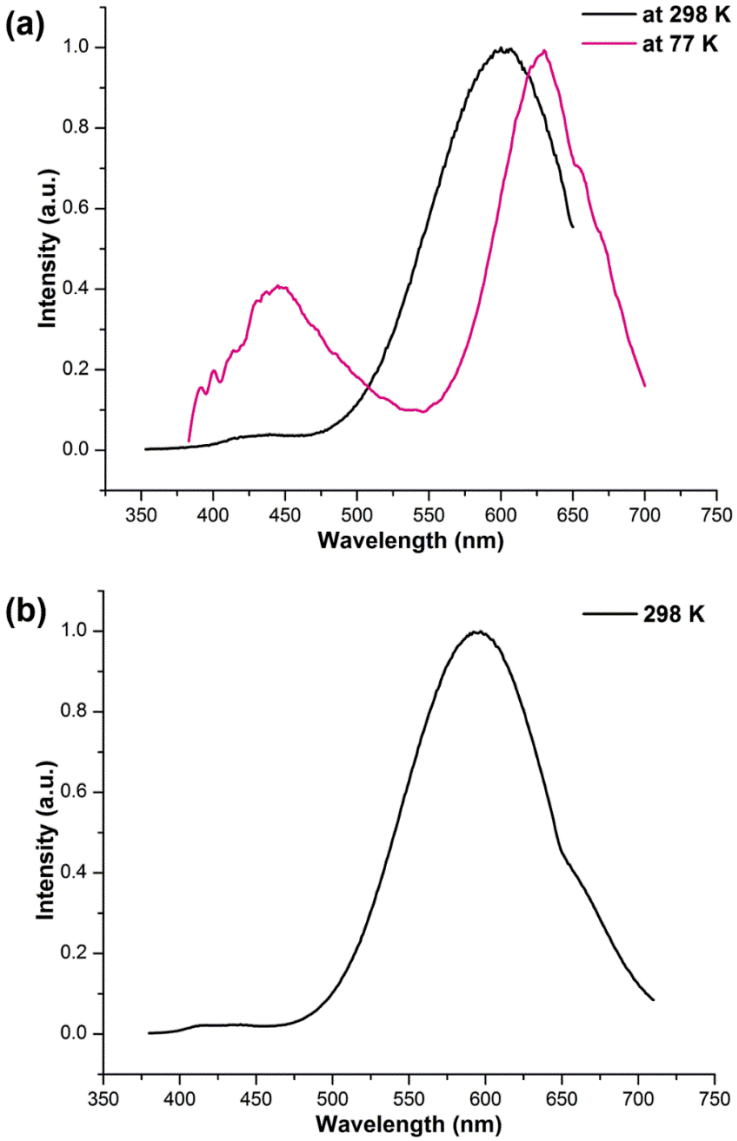

Figure 19: Solid-state emission spectra of (a) complex **1** at 298 K & 77 K and (b) complex **2** at 298 K.

Solid-state UV-Vis spectra

Further, the optical properties of the compounds **1**, **2**, **3**, **4** and **5**, were probed by the solid UV-Vis spectra which are shown below in figure 20. The compounds **1** and **2** show the absorption spectra typical of the cubane-type $Cu_4I_4L_4$ clusters exhibiting a ligand centered

emission at around 310 nm and the cluster centered emission characteristic of ^{1}XLCT transition at 430 nm.

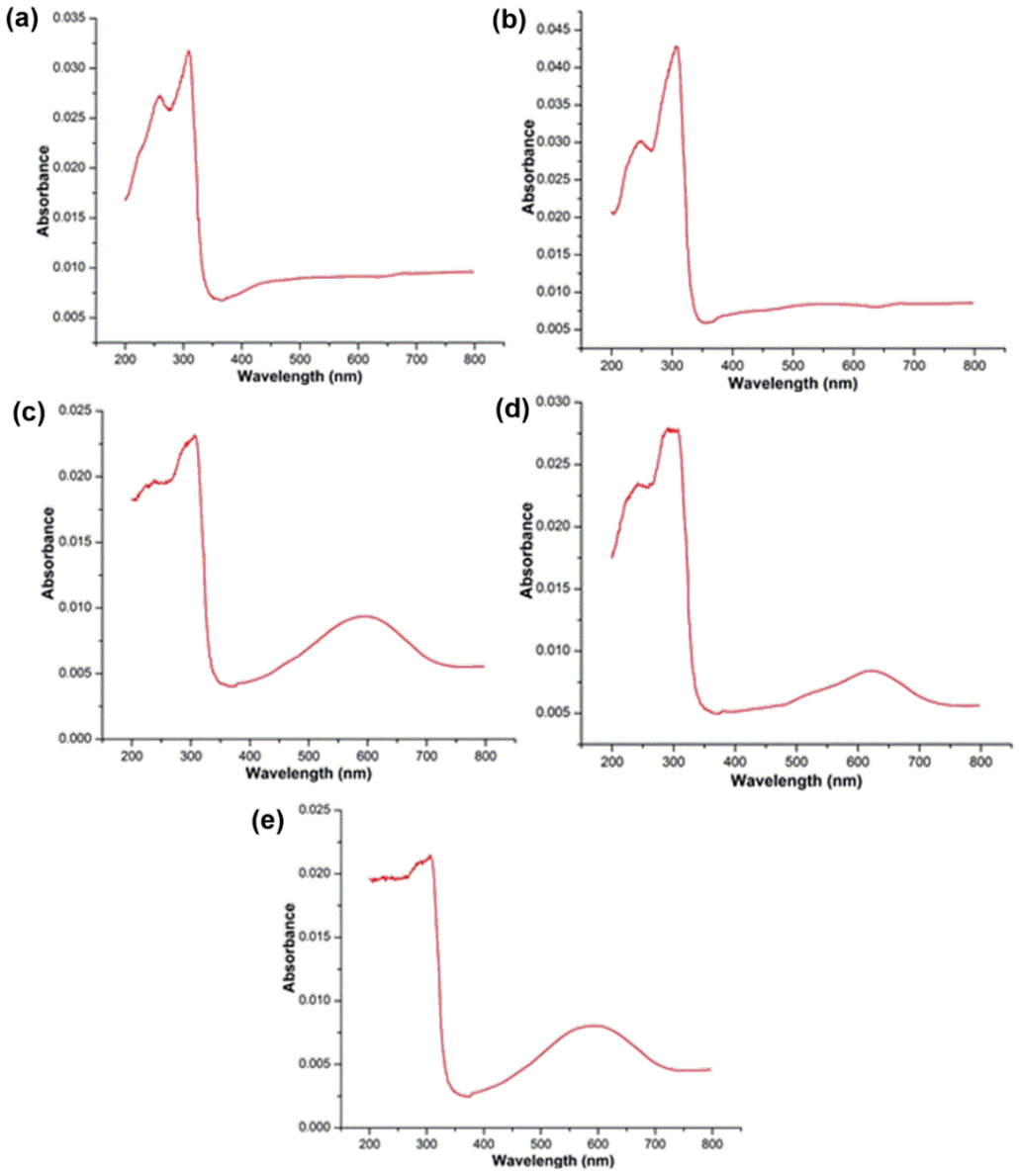

Figure 20: Solid UV-Vis spectra of (a) complex **1**, (b) complex **2**, (c) complex **3**, (d) complex **4** and (e) complex **5**.

Interestingly, the oxido clusters **3**, **4** and **5** show a low energy cluster centered absorption at around 600 nm. This feature of these clusters is responsible for their intense colors at the ambient light. Thus, the compound **3** shows dark brownish yellow color, **4** shows intense brown and **5** exhibiting brownish yellow color.

Photocatalysis: Methylene blue degradation

Methylene blue is a cationic dye which is mostly used for dyeing cotton wools, coloring paper, hair colorant, etc. Although MB is not considered to be a very toxic dye, its effects are very harmful to living things. Symptoms after inhaling MB in human beings can be difficulties in breathing, vomiting, diarrhea, and nausea, etc.[19, 20]

The molecular formula of MB is $C_{16}H_{18}N_3SCl$, and its IUPAC name is 3,7-bis(Dimethylamino)-phenothiazin-5-ium chloride. The structural of MB is shown below in figure 21.

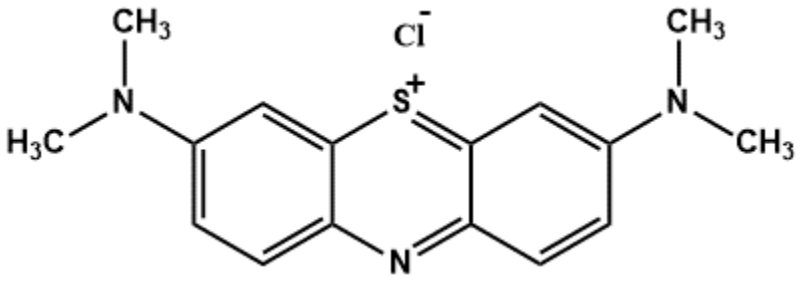

Figure 21: Structure of Methylene blue (MB).

A considerable amount of total world production of dyes is lost during the dyeing process which is released in the textile effluents resulting increase in the level of pollution and hence perturbations in the aquatic life.[21] Removal of such organic pollutants is important, and degradation is one of the top methods used for it.

In this effort, we have studied the photocatalytic activity of the synthesized complexes **1**, **2**, **3**, **4** and **5** to degrade the methylene blue (**MB**) in heterogeneous suspensions in the presence of H_2O_2.

Complex 1: At room temperature, 9.69 mg of complex **1** (5 ppm) was added into 6 ml of 50 mgL^{-1} (0.3 mg) methylene blue solution in water. 0.5 ml of the reaction solution was diluted into 4 ml, and 7 such samples were prepared. Then 30% H_2O_2 solution (0.1 ml) was injected in the each of the above solutions. Afterward, the prepared suspensions were exposed to the 200 W daylight lamp for the different time period (i.e. 0 min, 5 min,

10 min, 15 min, 20 min, 25 min and 30 min). Observed colors for each time period is shown in figure 22a.

Complex 2: At room temperature, 9.69 mg of complex **2** (5 ppm) was added to 6 ml of 50 mgL^{-1} (0.3 mg) methylene blue solution in water. 0.5 ml of the reaction solution was diluted with 4 ml, and 7 such samples were prepared. Then 30% H_2O_2 solution (0.1 ml) was injected in the each of the above solutions. Afterward, the prepared suspensions were exposed to the 200 W daylight lamp for the different time period (i.e. 0 min, 5 min, 10 min, 15 min, 20 min, 25 min and 30 min). Observed colors for each time period is shown in figure 22b.

Complex 3: At room temperature, 8.26 mg of complex **3** (5 ppm) was added to 6 ml of 50 mgL^{-1} (0.3 mg) methylene blue solution in water. 0.5 ml of the reaction solution was diluted with 4 ml, and 7 such samples were prepared. Then 30% H_2O_2 solution (0.1 ml) was injected in the each of the above solutions. Afterward, the prepared suspensions were exposed to the 200 W daylight lamp for the different time period (i.e. 0 min, 5 min, 10 min, 15 min, 20 min, 25 min and 30 min). Observed colors for each time period is shown in figure 22c.

Complex 4: At room temperature, 9.63 mg of complex **4** (5 ppm) was added to 6 ml of 50 mgL^{-1} (0.3 mg) methylene blue solution in water. 0.5 ml of the reaction solution was diluted with 4 ml, and 7 such samples were prepared. Then 30% H_2O_2 solution (0.1 ml) was injected in the each of the above solutions. Afterward, the prepared suspensions were exposed to the 200 W daylight lamp for the different time period (i.e. 0 min, 5 min, 10 min, 15 min, 20 min, 25 min and 30 min). Observed colors for each time period is shown in figure 22d.

Complex 5: At room temperature, 11.04 mg of complex **5** (5 ppm) was added to 6 ml of 50 mgL^{-1} (0.3 mg) methylene blue solution in water. 0.5 ml of the reaction solution was diluted with 4 ml, and 7 such samples were prepared. Then 30% H_2O_2 solution (0.1 ml) was injected in the each of the above solutions. Afterward, the prepared suspensions were exposed to the 200 W daylight lamp for the different time period (i.e. 0 min, 5 min, 10 min, 15 min, 20 min, 25 min and 30 min). Observed colors for each time period is shown in figure 22e.

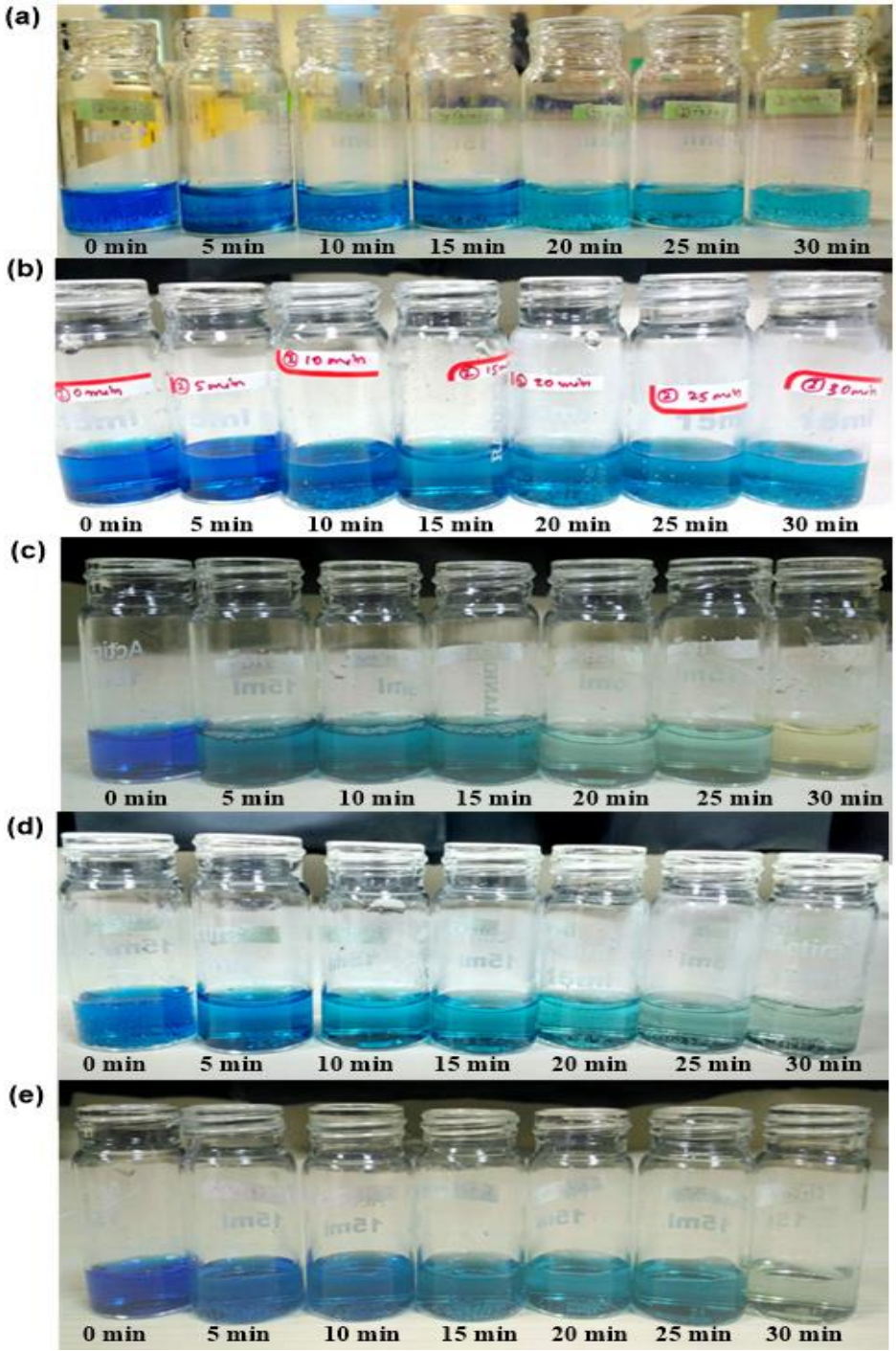

Figure 22: The **MB** solution faded under Visible Light with the catalysis of (a) complex **1**, (b) complex **2**, (c) complex **3**, (d) complex **4** and (e) complex **5** in the presence of H_2O_2.

The diluted reaction solutions were filtered, and their absorbance was measured using a UV-Vis spectrophotometer (shown in figure 23).

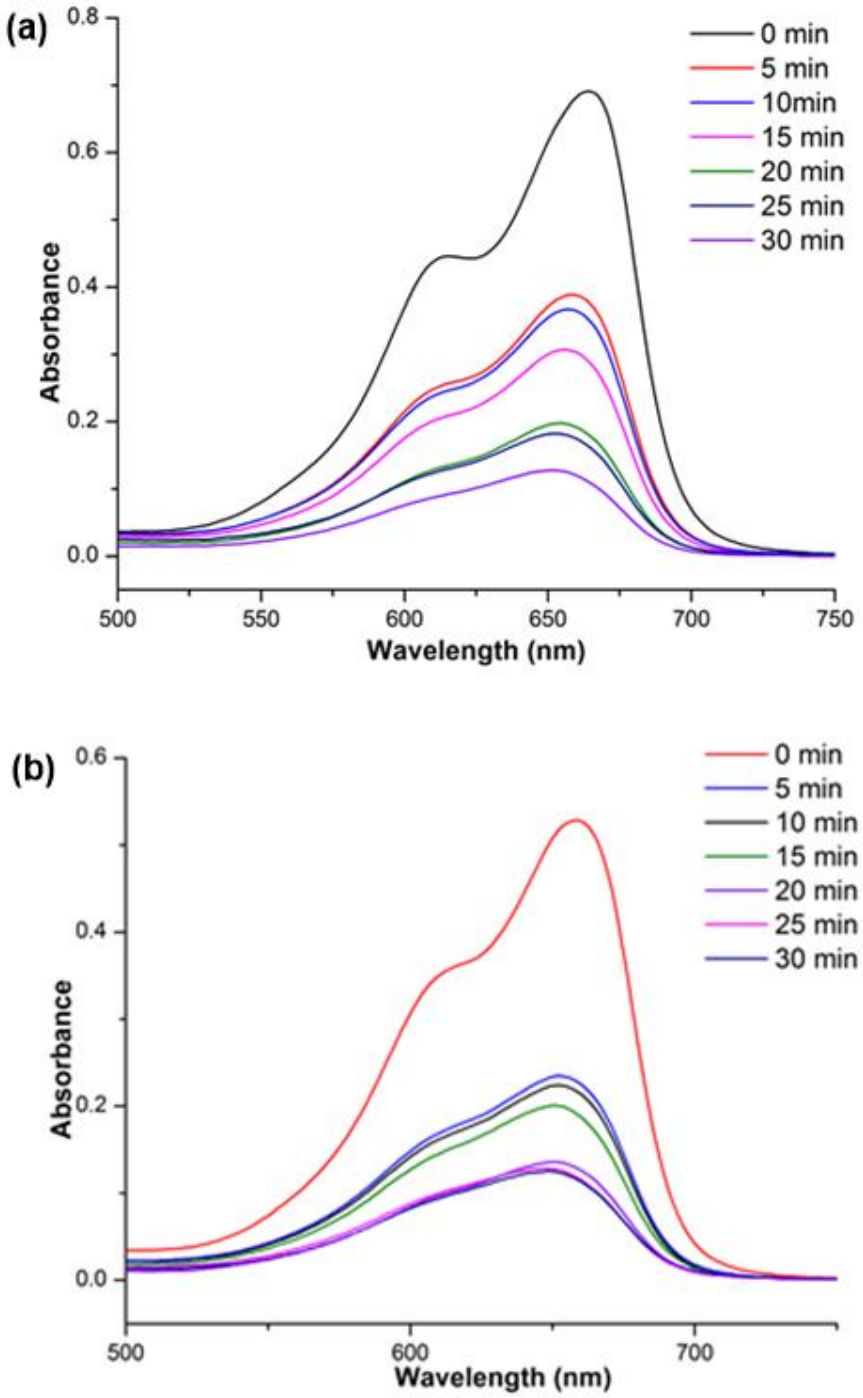

Figure 23: UV-Vis absorption spectrum changes of **MB** aqueous solutions with the photo-degradation catalyzed by H_2O_2 and (a) complex **1** and (b) complex **2**.

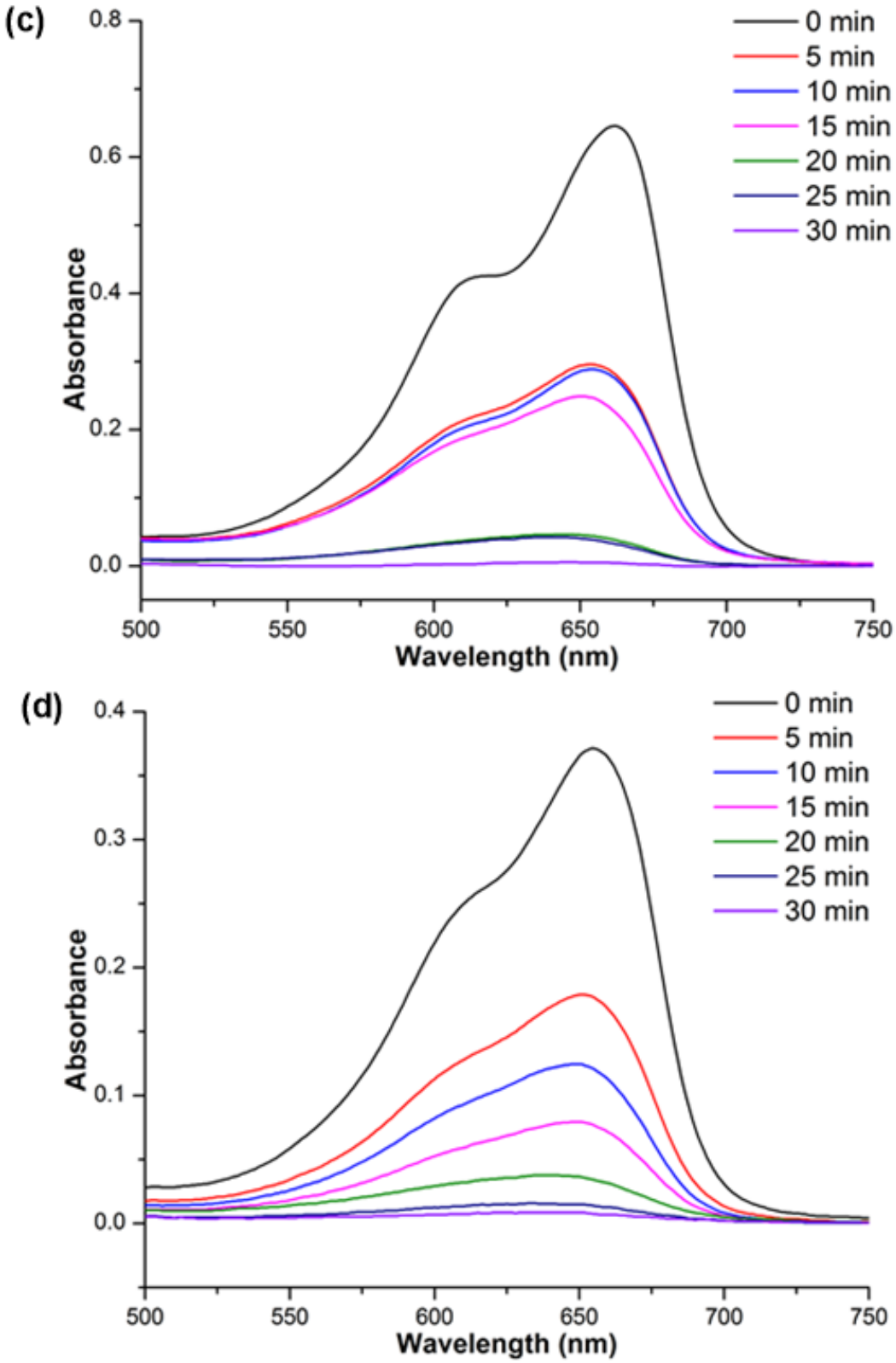

Figure 23: UV-Vis absorption spectrum changes of **MB** aqueous solutions with the photo-degradation catalyzed by H_2O_2 and (c) complex **3** and (d) complex **4**.

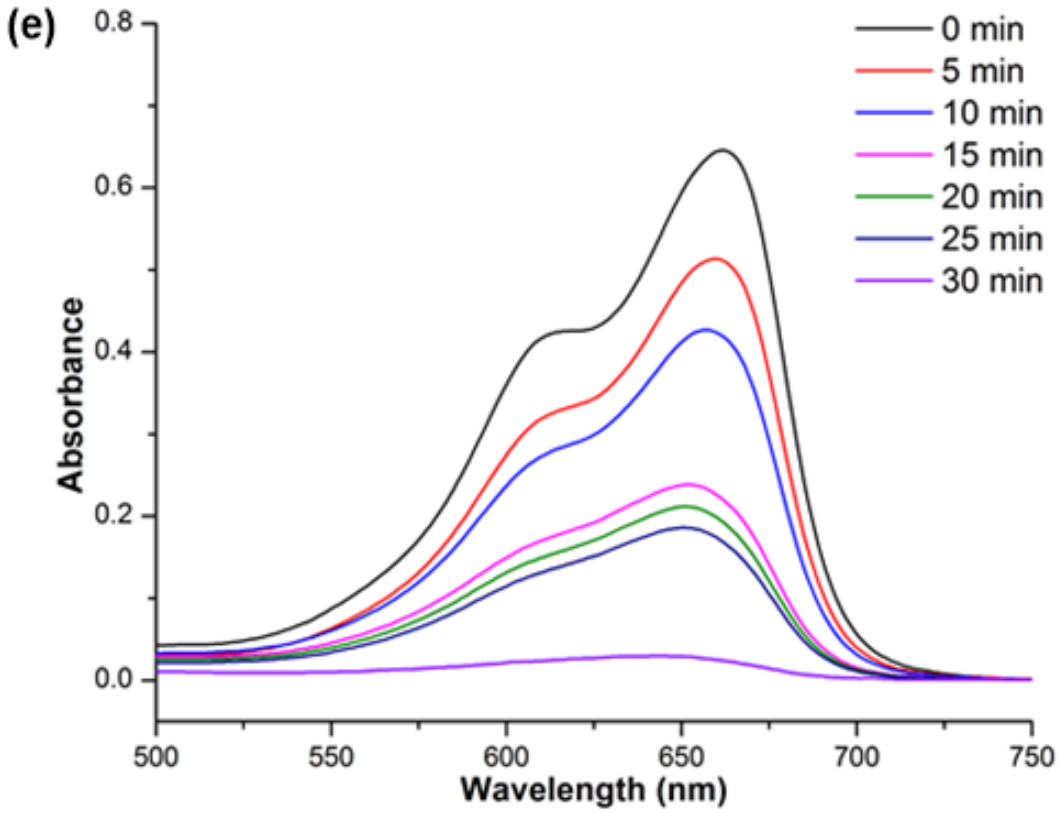

Figure 23: UV-Vis absorption spectrum changes of **MB** aqueous solutions with the photo-degradation catalyzed by H_2O_2 and (e) complex **5**.

As shown in the above UV-Vis spectra for the photodegradation experiment in the presence of complex **1**, **2**, **3**, **4** and **5** in the presence of H_2O_2, the characteristic absorbance of methylene blue (MB) at about 665 nm gradually degrades with increasing time from 0 to 30 min. All complexes act as good photocatalyst, as the absorbance decreases with time in all of the spectra, while in the case of complex **3**, **4** & **5** the absorbance of **MB** almost degraded to zero. As discussed earlier, complex **3**, **4** & **5** are the very rare type of self-assembly with copper halides having O^{2-} ion inside. Moreover, their photocatalytic activity to degrade MB under visible light in the presence of H_2O_2 is excellent.

For the quantitative comparison of the degradation by the complexes, the graph of the % quenching vs. time was plotted and has been shown in figure 24.

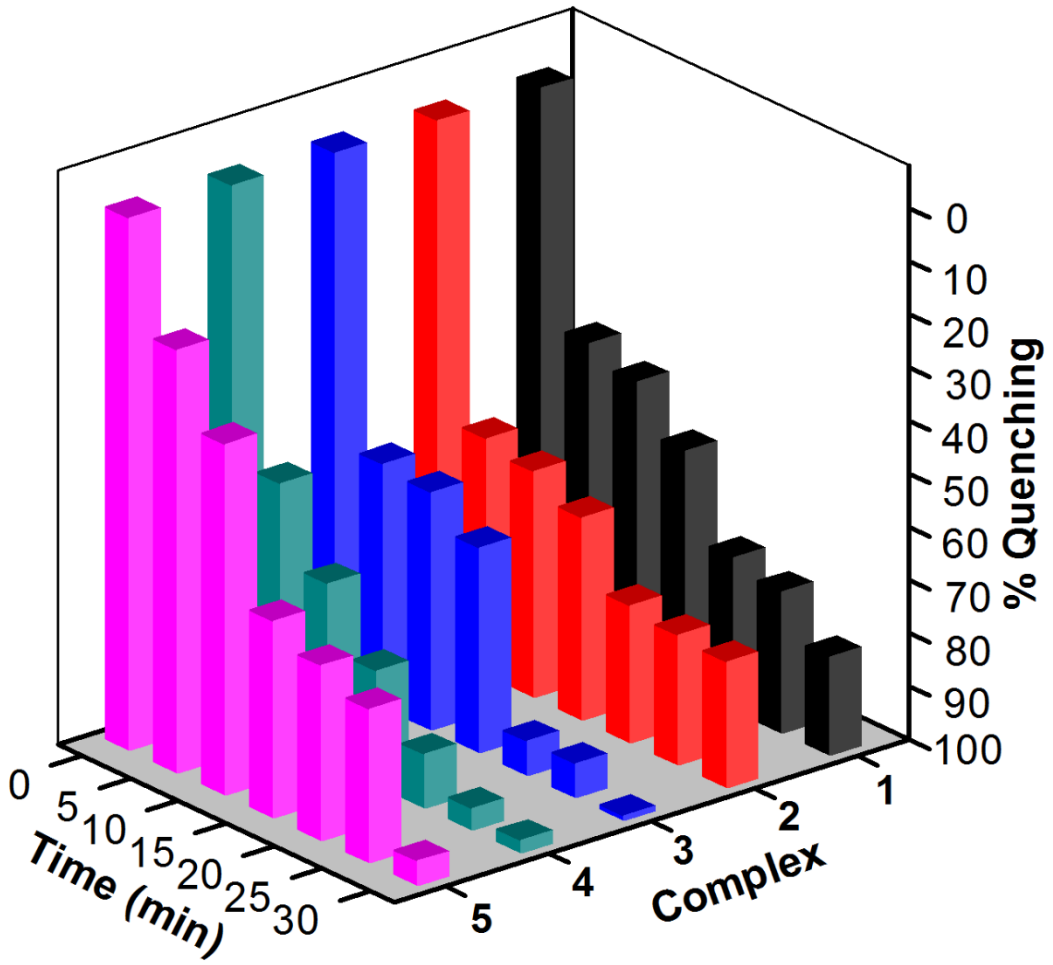

Figure 24: A Bar graph showing % quenching of MB by complexes **1, 2, 3, 4** and **5**.

From the graph, it can be seen that the percentage quenching of MB in the case of complex **1** and **2** were around 81.6% and 76.4%, respectively. Whereas in the case of the oxido clusters its was found to be 99%, 97.4% and 95.5 % for **3**, **4** and **5**, respectively exemplifying that the oxido clusters act as much better catalysts for MB degradation in the presence of H_2O_2.

PXRD

The stability of the complexes **1**, **2**, **3**, **4** and **5** after MB degradation was confirmed by PXRD experiments. The obtained PXRD patterns were shown in figure 25.

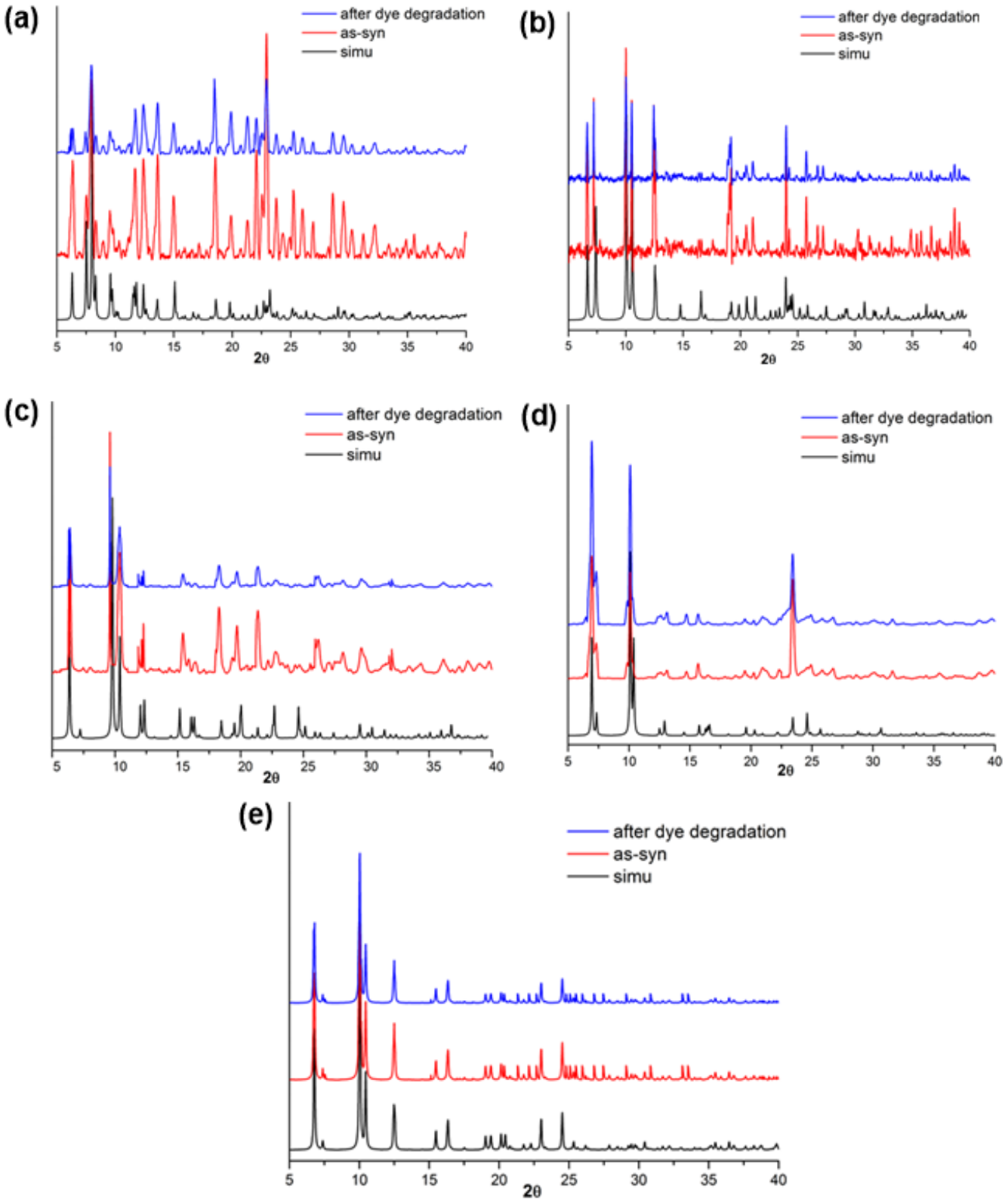

Figure 25: PXRD patterns of (a) complex **1**, (b) complex **2**, (c) complex **3**, (d) complex **4** and (e) complex **5**.

As it can be seen in figure 24, the PXRD patterns of all the synthesized complexes **1**, **2**, **3**, **4** and **5** are matching with the reference powder pattern obtained from the crystal structure. Also, these complexes are stable after the methylene blue degradation experiment which can clearly be seen from the PXRD pattern after dye degradation, which confirms that these complexes are acting as a catalyst in MB degradation at room temperature in the presence of H_2O_2.

Mechanism

As explained in the section of UV-Vis spectra, all complexes **1**, **2**, **3**, **4** and **5** show a ligand-centric transition at around 310 nm. $Cu_4I_4L_4$ clusters **1** and **2** show a small peak at around 430 nm due to cluster-centric ^{3}XLCT transition. Notably, the oxido clusters **3**, **4** and **5** show a low energy cluster-centric transition at around 600 nm in addition to ligand-centric transition. It is expected that all these complexes in the presence of visible light release energy due to their triplet state ligand-centric transition which is used to generate hydroxyl radicals from H_2O_2.[22] Simplified mechanism of MB degradation is shown in figure 26a.

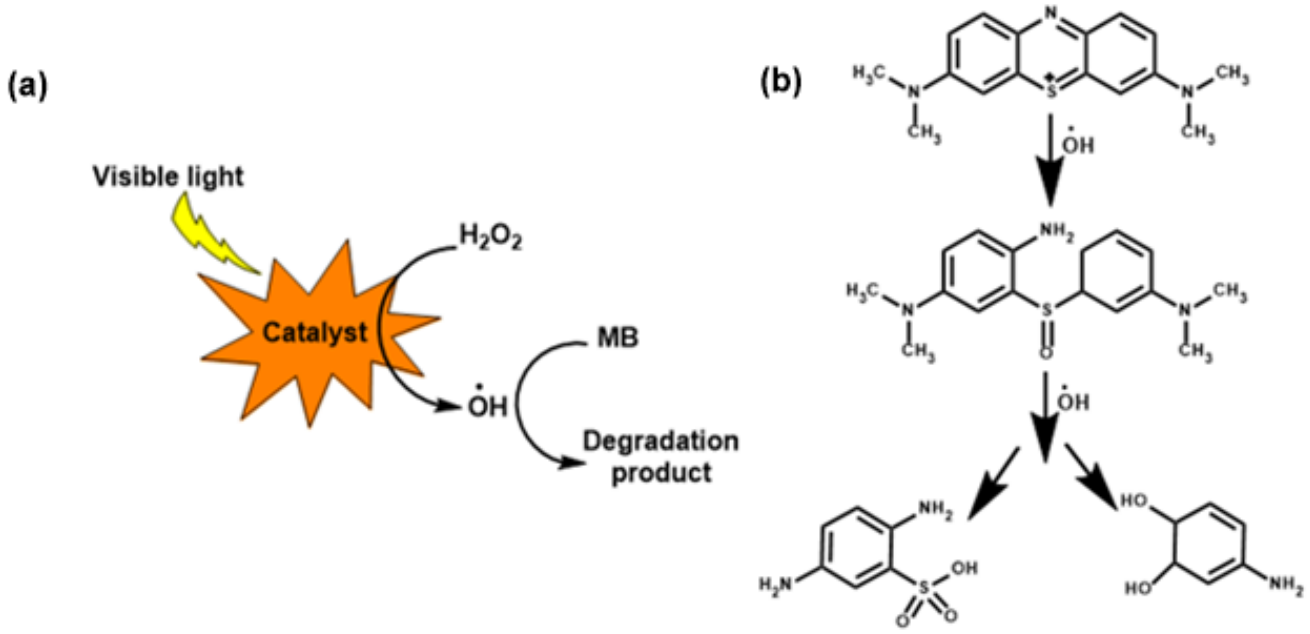

Figure 26: (a) Simplified mechanism of MB degradation and (b) Decomposition of MB in the presence of hydroxide radical.

The hydroxyl radical produced is attracted towards the cationic sulfur in MB through electrophilic interaction inducing the opening of the aromatic ring to produce sulphoxides and hydrated amino products.[23] Decomposition of MB through hydroxyl radical is shown in figure 26b. However, the exact mechanism is yet to be studied in future. In the case of oxido clusters **3**, **4** and **5**, the energy released is more due to the additional low energy cluster-centric transitions at 600 nm facilitating the production of hydroxyl radical and hence the better MB degradation compared to **1** and **2**. This property of oxido clusters makes them as an excellent photocatalyst for MB degradation.

Conclusion

In summary, I have synthesized two isostructural monodentate ligands **L^1** and **L^2** containing P-N bond which was then reacted with copper (I) iodide, copper (I) bromide and copper (II) chloride dehydrate to obtain two kinds of self-assembled discrete clusters Cu_4I_4 with **L^1** and **L^2** and Cu_4X_6O with **L^2** (X = Cl, Br, & I) at various conditions. Cu_4I_4 type clusters **1** and **2** are found to have thermochromic luminescence behavior and are red shifted on cooling from 298 K to 77 K. Obtained Cu_4X_6O clusters with **L^2** are the rare type of self-assembly with copper halides. These clusters have O^{2-} ion inside and their luminescence is quenched. Further, the photocatalytic activity of all of the complexes was studied by methylene blue degradation experiment. It was found that all of these complexes were able to degrade methylene blue in the presence of H_2O_2 at room temperature. Complex **1** and **2** were able to degrade MB at around 81.6% and 76.4% respectively while in the case of oxido clusters degradation of MB was found to be 99%, 97.4% and 95.5 % for **3**, **4** and **5** respectively in 30 minutes. Further, the stability of the complexes after dye degradation was confirmed by PXRD. Hence, all of the complexes **1**, **2**, **3**, **4** and **5** show very good photocatalytic activity. Moreover, **3**, **4** and **5** are excellent photocatalysts.

References

1. (a) Cariati, E.; Macchi, R.; Roberto, D.; Ugo, R.; Galli, S.; Casati, N.; Macchi, P.; Sironi, A.; Bogani, L.; Caneschi, A. *J. Am. Chem. Soc.* **2007,** *129,* 9410−9420. (b) Horcajada, P.; Serre, C.; Vallet-Regí, M.; Sebban, M.; Taulelle, F.; Fé rey, G. *Angew. Chem., Int. Ed.* **2006,** *45,* 5974−5978. (c) Ma, L.; Falkowski, J. M.; Abney, C.; Lin, W. *Nat. Chem.* **2010,** *2,* 838−846. (d) Wang, M.-S.; Guo, S.-P.; Li, Y.; Cai, L.-Z.; Zou, J.-P.; Xu, G.; Zhou, W.-W.; Zheng, F.-K.; Guo, G.-C. *J. Am. Chem. Soc.* **2009,** *131,* 13572−13573.

2. (a) Batten, S. R.; Murray, K. S. *Coord. Chem. Rev.* **2003,** *246,* 103−130. (b) Noveron, J. C.; Lah, M. S.; Del Sesto, R. E.; Arif, A. M.; Miller, J. S.; Stang, P. J. *J. Am. Chem. Soc.* **2002,** *124,* 6613−6625. (c) Wang, X.-Y.; Wang, Z.-M.; Gao, S. *Chem. Commun*. **2007**, 1127−1129.

3. (a) Gupta, A. K.; Srivastava, A. K.; Mahawar, I. K.; Boomishankar, R. *Cryst. Growth Des.* **2014,** *14,* 1701−1709. (b) Srivastava, A. K.; Praveenkumar, B.; Mahawar, I. K.; Divya, P.; Shalini, S.; Boomishankar, R. *Chem. Mater*. **2014**, *26,* 3811−3817. (c) Gupta, A. K.; Yadav, A.; Srivastava A. K.; Ramya, K. R.; Paithankar, H.; Nandi, S.; Chugh, J.; Boomishankar, R. *Inorg. Chem.* **2015,** *54,* 3196−3202. (d) Li, N.; Jiang, F.; Chen, L.; Li, X.; Chen, Q.; Hong, M. *Chem. Commn.* **2011**, *47,* 2327−2329. (e) Li, X.-J.; Jiang, F.-L.; Wu, M.-Y.; Zhang, S.-Q.; Zhou, Y.-F.; Hong, M.-C. *Inorg. Chem.* **2012,** *51,* 4116−4122 (f) Yadav A.; Srivastava A. K.; Balamurugan A.; Boomishankar R.; *Dalton Trans*., **2014**, *43*, 8166–816.

4. Yadav, A.; Boomishankar, R. *RSC Adv.,* **2015**, *5*, 3903 –3907.

5. (a) Pang, J.; Marcotte, E. J. P.; Seward, C.; Brown, R. S.; Wang, S. *Angew. Chem., Int. Ed*. **2001**, *40*, 4042−4045. (b) Keefe, M. H.; Benkstein, K. D.; Hupp, J. T. *Coord. Chem. Rev.* **2000**, *205*, 201−228. (c) McLaurin, E. J.; Vlaskin, V. A.; Gamelin, D. R. *J. Am. Chem. Soc.* **2011**, *133*, 14978−14980. (d) Cui, Y.; Xu, H.; Yue, Y.; Guo, Z.; Yu, J.; Chen, Z.; Gao, J.; Yang, Y.; Qian, G.; Chen, B. *J. Am. Chem. Soc.* **2012**, *134*, 3979−3982. (e) Uchiyama, S.; Kawai, N.; de Silva, A. P.; Iwai, K. *J. Am. Chem. Soc.* **2004**, *126*, 3032−3033.

6. (a) Choi, S. J.; Kuwabara, J.; Nishimura, Y.; Arai, T.; Kanbara, T. *Chem. Lett*. **2012**, *41*, 65 −67. (b) Kozhevnikov, V. N.; Donnio, B.; Bruce, D. W. *Angew. Chem., Int. Ed*. **2008**, *47*, 6286−6289. (c) Ito, H.; Saito, T.; Oshima, N.; Kitamura, N.; Ishizaka, S.; Hinatsu, Y.; Wakeshima, M.; Kato, M.; Tsuge, K.; Sawamura, M. *J. Am. Chem. Soc*. **2008**, *130*,

10044−10045. (d) Lee, Y.-A.; Eisenberg, R*. J. Am. Chem. Soc*. **2003**, *125*, 7778−7779. (e) Laguna, A.; Lasanta, T.; López*de*-Luzuriaga, J. M.; Monge, M.; Naumov, P. e.; Olmos, M. E. *J. Am. Chem. Soc.* **2009**, *132*, 456−457. (f) Dias, H. R.; Diyabalanage, H. V.; Rawashdeh-Omary, M. A.; Franzman, M. A.; Omary, M. A*. J. Am. Chem. Soc.* **2003**, *125*, 12072− 12073.

7. (a) Malwitz, M. A.; Lim, S. H.; White-Morris, R. L.; Pham, D. M.; Olmstead, M. M.; Balch, A. L. *J. Am. Chem. Soc.* **2012**, *134*, 10885− 10893. (b) Lefebvre, J.; Batchelor, R. J.; Leznoff, D. B. *J. Am. Chem. Soc.* **2004**, *126*, 16117−16125. (c) Ni, J.; Zhang, L.-Y.; Wen, H.-M.; Chen, Z.-N. *Chem. Commun.* **2009**, 3801−3803. (d) Wadas, T. J.; Wang, Q.-M.; Kim, Y.-j.; Flaschenreim, C.; Blanton, T. N.; Eisenberg, R. *J. Am. Chem. Soc.* **2004**, *126*, 16841−16849.

8. (a) Baleizao, C.; Nagl, S.; Schäferling, M.; Berberan-Santos, M. N.; Wolfbeis, O. S. *Anal. Chem.* **2008**, *80*, 6449−6457. (b) Wang, X.d.; Wolfbeis, O. S.; Meier, R. *J. Chem. Soc. Rev*. **2013**, *42*, 7834−7869. (c) Nagura, K.; Saito, S.; Yusa, H.; Yamawaki, H.; Fujihisa, H.; Sato, H.; Shimoikeda, Y.; Yamaguchi, S. *J. Am. Chem. Soc.* **2013**, *135*, 10322−10325. (d) Sage, I.; Badcock, R.; Humberstone, L.; Geddes, N.; Kemp, M.; Bourhill, G. *Smart Mater. Struct*. **1999***, 8*, 504. (e) Sage, I.; Bourhill, G. *J. Mater. Chem*. **2001**, *11*, 231−245.

9. Kyle, K. R.; Ryu, C. K.; Ford, P. C.; DiBenedetto, J. A. *J. Am. Chem. Soc.* **1991**, *113*, 2954−2965.

10. Parmeggiani F.; Sacchetti A. *J. Chem. Educ.* **2012**, *89*, 946−949.

11. (a) Ford, P. C.; Cariati, E.; Bourasssa*, J. Chem. Rev.* **1999**, *99*, 3625−3647. (b) Yam, V. W.-W.; Lo, K.K.-W. *Chem.Soc. Rev.* **1999**, *28*, 323−334. (c) Barbieri, A.; Accorsi, G.; Armaroli, N*. Chem. Commun*. **2008**, 2185−2193.

12. Perruchas, S.; Tard, C.; Le Goff, X. F.; Fargues, A.; Garcia, A.; Kahlal, S.; Saillard, J.-Y.; Gacoin, T.; Boilot, J.-P*. Inorg. Chem*. **2011**, *50*, 10682−10692.

13. Sagara, Y.; Mutai, T.; Yoshikawa, I.; Araki, K. *J. Am. Chem. Soc.* **2007**, *129*, 1520−1521.

14. (a) Perruchas, S.; Le Goff, X. F.; Maron, S.; Maurin, I.; Guillen, F.; Garcia, A.; Gacoin, T.; Boilot, J.-P. *J. Am. Chem. Soc*. **2010**, *132*, 10967−10969. (b) Benito, Q.; Le Goff, X. F.; Maron, S.; Fargues, A.; Garcia, A.; Martineau, C.; Taulelle, F.; Kahlal, S.; Gacoin, T.; Boilot, J.-P.; Perruchas, S. *J. Am. Chem. Soc.* **2014**, *136*, 11311−11320. (c) Wen, T.; Zhang, D.-X.; Liu, J.; Lin, R.; Zhang, J. *Chem. Commun.* **2013**, *49*, 5660−5662. (d) Shan, X.-C.; Jiang, F.-L.; Chen, L.; Wu, M.-Y.; Pan, J.; Wan, X.Y.; Hong, M.-C. *J. Mater. Chem. C,* **2013**, *1*, 4339−4349.

15. (a) Ford, P. C. *Coord. Chem. Rev.* **1994**, *132*, 129−140. (b) Kyle, K. R.; Ryu, C. K.; Ford, P. C.; DiBenedetto, J. A. *J. Am. Chem. Soc.* **1991**, *113*, 2954−2965. (c) Sun, D.; Yuan, S.; Wang, H.; Lu, H.-F.; Feng, S.-Y.; Sun, D.-F. *Chem. Commun.* **2013**, *49*, 6152−6154.

16. Deshmukh M. S.; Yadav A.; Pant R.; Boomishankar R. *Inorg. Chem.*, **2015**, *54* , 1337–1345.

17. Liu J.; Wang F.; Liu L.-Y.; Zhang J. *Inorg. Chem*. **2016***, 55*, 1358−1360.

18. Borgens R. B.; Shi R.; Bym S. R.; Smith D. T. **Patent** Jun 2, **2011** *US 20110130429 A1*.

19. K. Pirkannicmi & M.Sillanpaa, *Chemosphere* **2002,** *48*, 1047.

20. Mohabansi N.P.;Patil V. B.;Yenkie N. Rasayan *J. Chem.* **2011**, *4*, 814-819.

21. Color Chemistry. Synthesis, Properties and Applications of Organic Dyes and Pigments, 2nd revised Edition, in H. Zollinger (Ed.), VCH, 1**991**.

22. Yang X.; Chen W.; Huang J.; Zhou Y.; Zhu Y.; Li C. *Scientific reports 5*, **2015**, 10632.

23. Chithambararaj A.; Sanjini N. S.; Bose C.; Velmathi S. Catal. Sci. Technol., **2013**, *3*, 1405-1414.